AN INVESTIGATION INTO THE REMOVAL OF ALUMINOSILICATES SCALING SPECIES BY ACTIVATED ALUMINA

By

Ndishavhelafhi Mbedzi

A thesis presented for the degree of Master of Science in Engineering

Department of Chemical Engineering

University of Cape Town

March 2010

I know the meaning of plagiarism and declare that all the work in this document, save for that which is acknowledged is my own.

ACKNOWLEDGEMENTS

Firstly, I would like to express my sincere gratitude to my supervisors, Prof. Alison Emslie Lewis and Mr Jeeten Nathoo for their unrelenting guidance and interest in this study.

To Dr Belinda Mcfadzean and Henry Matjie, thank you so much.

Appreciation is also articulated to the National Research Foundation, Sasol and the Department of Chemical Engineering for funding this research.

To my colleagues in the Crystallisation and Precipitation Unit, thank you. Working with you guys was fantastic.

To Riana Rossouw of the Geological Department at Stellenbosch University, Miranda Waldron of the Electron Microscope Unit (UCT) and Helen Divey from the Department of Chemical Engineering for the ICP-AES, SEM and AAS analyses respectively.

To my fiancé, Richard thank you for your encouragement and emotional support.

To my family and Ratie for all your prayers.

Sinetemba a.k.a Fresh you rock, you are my inspiration.

Last but not least, to the Almighty God, my fortress, my strength, the author and finisher of my life. Amen.

I would like to dedicate this to Cee, Ipfi, Unanne, my entire family and friends.

ABSTRACT

Gas condensates from the coal conversion plants contains trace amounts of inorganic species such as Si, Ca and Al ions, which cause scaling in downstream processes. Silica has been identified as the main constituent of the scale materials in geothermal plants. In order to prevent scaling, silica ions need to be removed or reduced. Alumina has been shown to successfully remove both silica and calcium from waste water streams. However, it also causes an increase in the aluminum concentration through dissolution.

The mechanism of the silica and calcium uptake by alumina is not fully understood. In this study, the mechanism of silica uptake by alumina was investigated through an extensive literature review and experimental work on the alumina and silica chemistry when in solution. The chemistry of the alumina in suspension can be used to explain its reactions with other species (both inorganic and organic) in solutions.

Activated alumina chemistry in suspension under alkaline conditions was investigated. The results showed that small amounts of alumina particles can undergo transformation into its hydrated phases and consequently aluminate ($Al(OH)_4^-$) species are leached out from the pellets and dissolve in solution with subsequent precipitation when in solution. The inorganic species uptake can be attributed to the species interacting with the Al in solution and the hydrated phases of alumina. The results on the inorganic species uptake by alumina showed that a break through point is never attained. This indicates that the inorganic species removal by alumina cannot be attributed exclusively to an adsorption process. Hence, the mechanism of species removal was suggested to be a combination of adsorption and surface precipitation/reaction.

Since alumina is costly, its application in wastewater treatment is dependent on its ability to be regenerated. As a result, the second objective of this study was to investigate the regeneration of the alumina by unloading the silica from the loaded alumina using various reagents and subsequently testing the effectiveness of the alumina with a second loading. The reagents used to unload the loaded alumina were sulphuric acid, sodium hydroxide and sodium gluconate at varying concentrations. The three reagents showed an increase in Si unloading with an increase in reagent concentrations. Sulphuric acid showed an unloading

capacity of up to about 50% and 70% for batch and continuous unloading respectively. On the other hand, sodium hydroxide showed Si unloading of up to about 50% and 40% for the batch and continuous unloading of loaded alumina respectively under the investigated concentrations. The unloading of Si from saturated alumina using sodium gluconate was only conducted batch-wise as it only achieved a 6% unloading for the concentrations investigated. However, even though the scaling species were eluted from the alumina bed this did not improve/restore the loading capacity of alumina but rather kept the performance of the alumina at the same level that it was before the regeneration process. Also during the unloading of silica from alumina, excessive alumina dissolution was observed when using 0.25M and 0.65M NaOH.

TABLE OF CONTENTS

ACKNOWLEDGEMENTS ..... **II**

ABSTRACT ..... **IV**

TABLE OF CONTENTS ..... **VI**

LIST OF FIGURES ..... **IX**

LIST OF TABLES ..... **XII**

1 INTRODUCTION 1

1.1 Background 1

1.2 Scope of the work 3

1.3 Objectives 3

2 THEORY AND LITERATURE REVIEW 4

2.1 Crystallization and precipitation fundamentals 4

2.1.1 Supersaturation 4

2.1.2 Nucleation 6

2.1.3 Crystal growth 7

2.1.4 Population balance 7

2.1.5 Scaling 8

2.2 Adsorption 9

2.2.1 Adsorption isotherms 9

2.2.2 Adsorbents 11

2.3 Alumina/aluminum oxide adsorbent 11

2.3.1 Alumina surface properties 12

2.3.2 Chemistry of alumina in aqueous systems 16

2.4 Silicon and aluminum 18

2.4.1 Dissolution of silica in solution 18

2.4.2 Hydrolysis of Al (III) in solution 20

2.5 Possible removal mechanisms of silicon species by alumina in solution 22

2.5.1 Adsorption and surface precipitation 23

2.5.2 Precipitation with the insoluble metal hydroxides and solubilised Al ions 25

2.5.3 Possible formation of aluminosilicates 26

2.6 Recovery of alumina loading capacity through dissolution of the aluminum silicate species 27
3 MATERIALS AND METHODS 29
3.1 Analytical techniques 29
3.2 Materials and chemicals 29
3.3 Experimental Design 30
3.4 Experimental program 32
3.4.1 Investigation into alumina surface chemistry in solution 32
3.4.2 Understanding the mechanisms of aluminum silicate species removal by alumina 34
3.4.3 Investigation into the unloading of the loaded bed of alumina 34
4 RESULTS AND DISCUSSION 36
4.1 Investigation into alumina surface chemistry in solution 36
4.1.1 Dissolution and transformation behaviour of alumina in suspension 36
4.1.2 Determination of activated alumina and silica zeta potential 41
4.2 Understanding the mechanism(s) of aluminum silicate species removal by activated alumina 42
4.3 Investigation into the unloading of the loaded bed of activated alumina by aluminum silicate species (regeneration) 50
4.3.1 Determination of the alumina-reagent ratio to be used 50
4.3.2 Investigations into the use of the various cleaning reagents to regenerate alumina 53
4.3.3 Regeneration of alumina in a continuous mode operation 57
4.3.4 Alumina loading capacity recovery 63
5 CONCLUSIONS 66
6 RECOMMENDATIONS 68
7 REFERENCES 69
8 APPENDICES 75
8.1 Appendix A: Raw data for aluminum dissolution in gas condensate 75
8.2 Appendix B: Particle size distribution 75
8.3 Appendix C: Raw data for silica zeta potential in 0.01M NaCl 78
8.4 Appendix D: Results for alumina loading with aluminosilicate species 79

8.5 Appendix E: Regeneration data for selected experiments to show calculations and reproducibility of the experimental results 81

LIST OF FIGURES

Figure 1: The X-ray fluorescence elemental analysis of the scaling material.....2
Figure 2: The role of supersaturation in precipitation processes (Sohnel and Garside, 1992).5
Figure 3: Effect of supersaturation on nucleation (Nielsen, 1979).....6
Figure 4: Effect of solid substrate to catalyse nucleation (Stumm, 1992).....7
Figure 5: The thermal transitional sequence of aluminum hydroxides to aluminas (Lippens and Steggerda, 1970; Ingram-Jones et al., 1996).....12
Figure 6: Idealized illustration of the cross section of the surface layer of a metal oxide (Goldberg et al., 1996; Stumm, 1992; Lippens and Steggerda, 1970).....13
Figure 7: Possible surface hydroxyl groups on aluminas (Peri, 1965; Kasprzyk-Horden, 2004).....15
Figure 8: Surface charge of alumina as a function of medium pH (Kasprzyk-Hordern, 2004) 17
Figure 9: Solubility-pH diagram for amorphous silica dissolution at 25°C and Ionic strength = 0.5.....20
Figure 10: Solubility-pH diagram of amorphous aluminium hydroxide hydrolysis at 25°C (Stumm and Morgan, 1996).....22
Figure 11: Interaction of silica and alumina resulting in an increase in surface area for further deposition of silica 24
Figure 12: Schematic diagram of the experimental system used for the continuous mode experiments.....32
Figure 13: Dissolution kinetics of activated alumina in deionised water at room temperature and pH adjusted at 8.3 to 9.0.....37
Figure 14: Dissolution kinetics of activated alumina in the gas condensate stream at room temperature and pH of 8.3 to 9.0 (2mg/l initial Al concentration).....37
Figure 15: Change in particle size diameter during alumina fines dissolution in water. 39
Figure 16: Particle size evolution during dissolution experiments.....40
Figure 17: XRD patterns of alumina suspended in deionised water for different times.....41
Figure 18: Zeta potential of alumina as a function of pH.....42
Figure 19: Zeta potential of silica as a function of pH.....42

Figure 20: Schematic summary of the most likely Si, Ca removal mechanism(s) by activated alumina with cumulative gas condensate volume....46
Figure 21: Concentrations of Si, Ca and Al in the synthetic solution contacted with activated alumina in a batch-wise mode as a function of time....47
Figure 22: Concentrations of Si, Ca and Al in gas condensate contacted with activated alumina in a batch-wise operation mode as a function of time....47
Figure 23: Concentrations of Si, Ca and Al in a continuously fed gas condensate through a packed bed of activated alumina (T=40°C, 6 minutes residence time)....48
Figure 24: Energy dispersive spectroscopy analysis of activated alumina pellets saturated with aluminum silicate species....49
Figure 25: Scanning Electron Microscopy photographs for activated alumina. A- Virgin alumina; B- alumina suspended in de-ionised water: C- alumina suspended in gas condensate....49
Figure 26: Percentage of Si, Ca, and Al removed from the gas condensate by virgin activated alumina (25g/L alumina dosage, 6 mins residence time)....51
Figure 27: Concentrations of Si in washing solution attained during batch-wise unloading of saturated activated alumina using 1 litre of 0.1M H_2SO_4 as a function of time (50g alumina)....52
Figure 28: Percentage of Si desorbed from a saturated bed of activated alumina during regeneration using different volumes of washing solution (0.1M H_2SO_4) as a function of time (50g alumina)....52
Figure 29: Concentrations of Si, Ca and Al in a continuously fed gas condensate through a packed bed of activated alumina (25g/l alumina dosage, 6 minutes residence time)....55
Figure 30: Percentage of Si, Ca, and Al removed from the gas condensate by virgin activated alumina (25g/L alumina dosage, 6 mins residence time)....56
Figure 31: Percentage of Si unloaded from loaded alumina at the end of the experiments for the various cleaning reagents for the different concentrations used (120 minutes reaction time).....56
Figure 32: Percentage of Al dissolved from the loaded alumina in the different cleaning reagents of varying concentrations at the end of the experiments (120 minutes reaction time)....57

Figure 33: Concentrations of Si, Ca and Al in a continuously fed gas condensate through a packed bed of activated alumina (25g/L alumina dosage, 6 minutes residence time) 58
Figure 34: Percentage of Si, Ca, and Al removed from the gas condensate by virgin activated alumina (25g/L alumina dosage, 6 mins residence time).....59
Figure 35: Concentrations of Si, Ca and Al in washing solution attained when using 0.1M H_2SO_4 to regenerate the loaded activated alumina as a function of time (3 minutes residence time).....59
Figure 36: Concentrations of Si, Ca and Al in washing solution attained when using 0.25M NaOH to regenerate the loaded activated alumina as a function of time (3 minutes residence time).....60
Figure 37: Concentrations of Si removed from loaded alumina in washing solution attained when using 0.1M H_2SO_4 and 0.25M NaOH to regenerate the loaded activated alumina as a function of time (3 minutes residence time).....60
Figure 38: Cumulative percentage Si unloaded from loaded alumina when regenerating loaded alumina using 0.1M H_2SO_4 and 0.25M NaOH (3 minutes residence time, and 50g loaded alumina).....61
Figure 39: Energy Dispersive Spectroscopy (EDS) analysis of fines formed during washing loaded alumina by 0.1M H_2SO_4 62
Figure 40: Scanning Electron Microscope photograph of the fines produced during washing of loaded alumina using 0.1M H_2SO_4 63
Figure 41: Concentrations of Si, Ca and Al in a continuously fed gas condensate through a packed bed of activated alumina previously washed using 0.1M H_2SO_4 (6 minutes residence time).....64
Figure 42: Percentage of Si, Ca and Al removed from gas condensate by loaded alumina which was previously washed using 0.1M H_2SO_4 (6 minutes residence time).....64
Figure 43: Concentrations of Si, Ca and Al in a continuously fed gas condensate through a packed bed of activated alumina previously washed using 0.25M NaOH (6 minutes residence time).....65
Figure 44: Percentage of Si, Ca and Al removed from gas condensate by loaded alumina which was previously washed using 0.25M NaOH (6 minutes residence time) 65
Figure 45: Concentrations of Si removed from loaded alumina in washing solution attained when using 0.1M H_2SO_4 for two different runs (3 minutes residence time).....84

LIST OF TABLES

Table 1: The desired theoretical concentrations of the synthetic solutions with respect to each aluminum silicate species 30

Table 2: Various concentrations of the different reagents used to regenerate saturated activated alumina 55

Table 3: The Energy Dispersive Spectroscopy (EDS) percentage element analysis of fines formed during washing of loaded alumina 62

Table 4: Al concentration in gas condensate during Al dissolution experiment collected as a function of time 75

Table 5: Excel spreadsheet for the conversion of volume distribution data to number distribution data obtained during dissolution experiments 76

Table 6: Silica zeta potentials obtained when using 0.01M NaCl 78

Table 7: Concentrations of Si, Ca and Al in gas condensate continuously fed through a packed bed of activated alumina 80

Table 8: Concentrations of Si, Ca and Al in gas condensate continuously fed through a packed bed of activated alumina 82

Table 9: Concentrations of Si, Ca and Al in liquid samples during continuous regeneration of loaded alumina with 0.1M H_2SO_4 83

1 INTRODUCTION

1.1 Background

Scaling is a major problem in industrial operations, especially in geothermal plants and power stations and hence its outstanding attention in the field of energy utilization (Yokoyama et al. 2002). The deposition of scaling compounds on the equipment surfaces reduces plant efficiencies as a result of frequent plant shut-downs for the removal of scale from the equipment. Chemical, mechanical and physical methods are used to prevent and reduce scaling in plants (Sohnel and Garside, 1992). Silica constitutes the greater part of the scaling material in geothermal plants (Matson, 1981). Several treatment techniques such as reverse osmosis, softening, ion exchange, demineralization and evaporation have been used to mitigate silica scaling in geothermal waters (Gallup et al., 2003; Matjie and Engelbrecht, 2007; Matson, 1981). Most techniques are not effective in removing silica because of the complexity of streams, as they are non-selective for example ion exchange (Matson, 1981). Chemical methods also result in formation of new compounds thereby creating other waste streams which have to be further treated prior to their disposal (Midkiff, 2002).

Precipitation and adsorption have been also used for the recovery and separation of both inorganic and organic species from solution (Frank, 2003; Ghorai and Pant, 2005; Gabelich et al., 2005). These have an advantage of being implemented even for species that are present in low concentrations in solution. Precipitation involves the formation of sparingly soluble solid phases from a liquid solution phase using a precipitating agent (Mullin, 1972). Adsorption is the adhesion of substances on a solid surface. Activated carbon is the most commonly used adsorbent for the removal of organic or inorganic species from the aqueous phase. The constantly increasing knowledge of alumina being gathered through research has found wide use of alumina industrially. One of alumina's uses in industry is as an adsorbent in waste-water streams containing fluoride, arsenic, selenium, thallium, beryllium and silica (Frank, 2003).

In this study, the feasibility of using alumina to remove/reduce scaling species and hence to mitigate silica scaling in geothermal plants was investigated. Coal being a natural resource contains elements such as silicon, iron and calcium. During coal conversion processes, trace

amounts of inorganic species such as Si, Ca, Al and Fe vaporize and are entrained in the gaseous phase (Matjie and Engelbrecht, 2007). A gas condensate containing these species is formed on cooling the gas phase.

During transportation of the gas condensate scaling occurs. Hydrofluoric acid and other toxic and corrosive chemicals have been employed to remove the scale material from the equipment at regular intervals (Matjie and Engelbrecht, 2007). Therefore, there is need for the development of affordable and less hazardous methods of reducing scaling.

Characterisation studies of the liquid samples identified metal ions such as Al^{3+}, Ca^{2+}, Fe^{3+}, Mg^{2+}, $Si^{4+}$and K^{+} (Matjie and Engelbrecht, 2007). The effective method to prevent the formation of scales is dependent on the reduction of the cationic concentrations (Peairs, 2007). The X-ray fluorescence (XRF) analysis results showed that silicon is the major component of the scale material as shown in Figure 1 (Matjie and Engelbrecht, 2007).

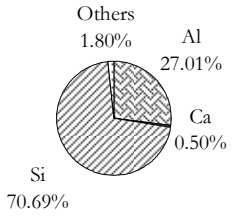

Figure 1: The X-ray fluorescence elemental analysis of the scaling material

As a result, the method to use must be the one which has high silicon removal efficiency. The technical feasibility of using alumina, silica gel and anthracite under batch and continuous operating conditions for the selective removal of the scaling cationic species from the gas condensate have been performed previously (Lewis and Nathoo, 2006). It was found that, within the experimental conditions investigated, alumina exhibited the best contaminant removal characteristics. However, the mechanism of species removal by the activated alumina is not fully understood. An understanding of the mechanism of species removal by activated alumina would enable the feasibility of using activated alumina to

remove the scaling species to be evaluated. Activated alumina is expensive and as a result, its application depends on the possibility of its regeneration.

1.2 Scope of the work

The overall scope of this study was to investigate the feasibility of using activated alumina to remove the scaling species, thereby reducing the scaling caused by Si, Al and Ca compounds (aluminosilicate species) in geothermal brines.

1.3 Objectives

The first objective of this study was to understand the mechanism(s) by which silicon species and calcium can be removed from multicomponent waste-waters by activated alumina. The study also focused on understanding the possible causes of the increase in the aluminum concentration in solution when alumina is being used to remove silicon species.

The second objective was to investigate the possibility of eluting silicon species and calcium from the loaded activated alumina bed using various reagents, thereby regenerating it. The performance of the regenerated alumina was then compared to its performance prior to regeneration.

The project was investigated in three sequential stages consisting of:

- Literature review to develop a better understanding of the most probable interactions of silicon species, calcium and alumina in solution. This was used to hypothesise likely mechanisms,
- A laboratory-based study to investigate the proposed mechanism(s),
- A study into identifying possible reagents and investigating their performance in unloading silicon species and calcium ions from the loaded alumina.

2 THEORY AND LITERATURE REVIEW

2.1 Crystallization and precipitation fundamentals

Crystallization is a separation technique used for the recovery of pure solids from impure solutions. The reactive form of crystallisation is referred to as precipitation (Stumm, 1992; Mullin, 1972). The difference in chemical potential at the actual (μ) and equilibrium (μ*) state gives the thermodynamic driving force for crystallisation (Δμ). Thus, the thermodynamic driving force can be expressed as follows:

$$\Delta\mu = \mu - \mu^* \tag{1}$$

For crystallisation to occur, Δμ must be positive (Sohnel and Garside, 1992). The driving force is also referred to as supersaturation (ΔC) which is expressed in terms of solute concentrations. The three key steps involved in precipitation processes are supersaturation, nucleation and crystal growth.

2.1.1 Supersaturation

Supersaturation (ΔC) is the difference between the actual solute concentration (C) and equilibrium solute concentration (C*) and it is dependent on system temperature and pressure. Thus, for a system at constant temperature and pressure, the supersaturation can be expressed as follows:

$$\Delta C = C - C^* \tag{2}$$

At times relative supersaturation σ is used and it is expressed as follows:

$$\sigma = \frac{\Delta C}{C^*} = S - 1 \tag{3}$$

, where $S = \frac{C}{C^*}$

Supersaturation plays a key role in precipitation processes as depicted in Figure 2.

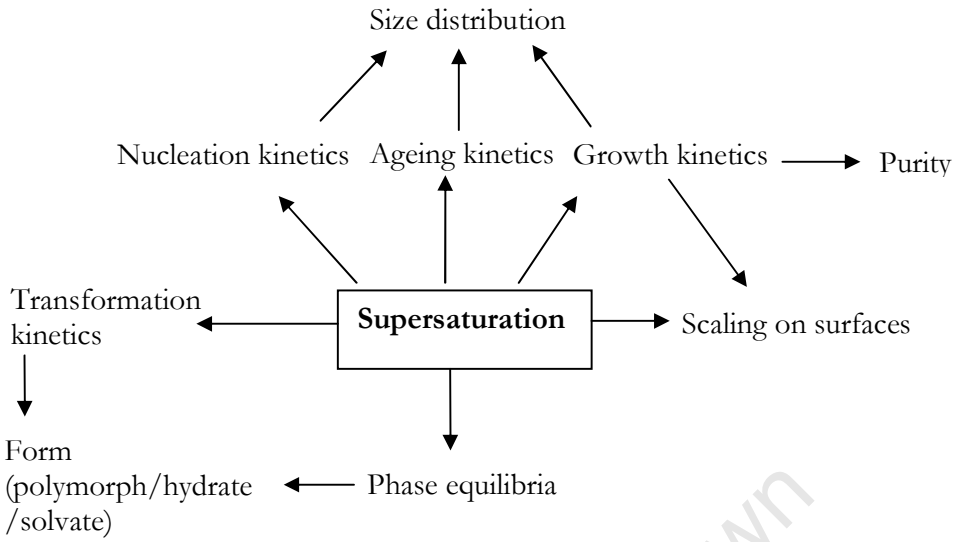

Figure 2: The role of supersaturation in precipitation processes (Sohnel and Garside, 1992)

The degree of supersaturation in the precipitating solution governs the rates of the different processes involved in precipitation (Nielsen, 1979). Figure 3 shows the different zones where the different particle formation mechanisms occur when species A and B are mixed as a result of the differences in supersaturation level. When the precipitation processes are not desirable, Zone 1 (the undersaturated region) is the ideal zone for operation since it is located below the solubility limit of AB. Zone 2 and 3 are the most preferred zones of operation for precipitation processes to occur. However, zone 4 and 5 are the least desirable operation regions as the solids formed under these regions present problems in downstream separation processes like filtration.

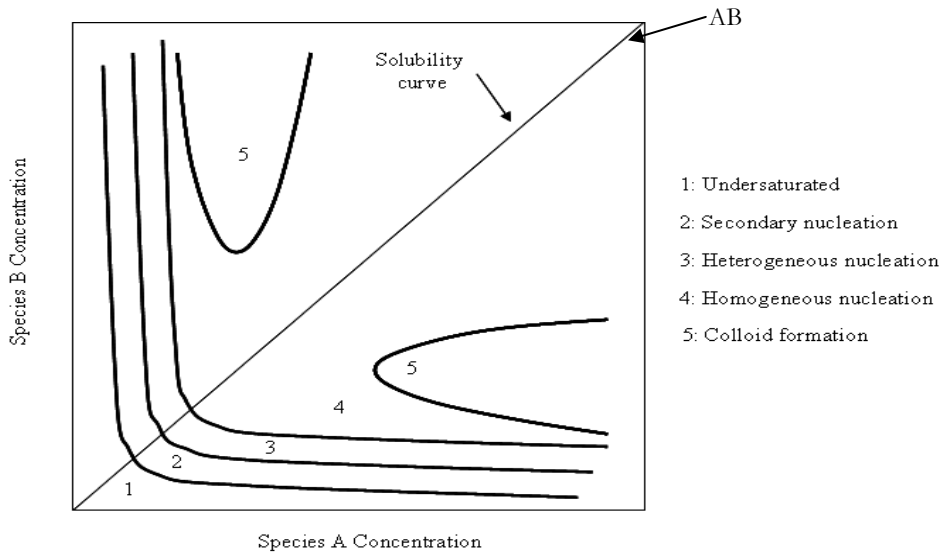

Figure 3: Effect of supersaturation on nucleation (Nielsen, 1979)

2.1.2 Nucleation

As solution supersaturation increases, a point is reached where ions or molecules interact to form thermodynamically stable solid particles (nuclei) (Stumm, 1992). This process is termed nucleation and it determines the size and distribution of particles in precipitation processes (Stumm, 1992; Myerson, 2002). There are chiefly two different types of nucleation namely primary and secondary nucleation. The former occurs in the absence of crystals and can be further broken down into homogeneous and heterogeneous nucleation. Homogeneous nucleation is supersaturation driven and not dependent upon the presence of solid particles. However, when foreign solids are present in solution nuclei are formed through heterogeneous nucleation (Mersmann, 2001; Stumm, 1992). The compatibility between the surfaces of foreign particle and the solution crystals reduces the energy barrier thereby catalysing the nucleation process as shown in Figure 4 (Stumm, 1992). On the other hand, secondary nucleation occurs even at low supersaturation if the solution contains parent crystals (Mersmann, 2001; Stumm, 1992; Mullin, 1972). Once a thermodynamically stable nucleus is formed, the nuclei and ions or molecules join together to form bigger particles (crystals).

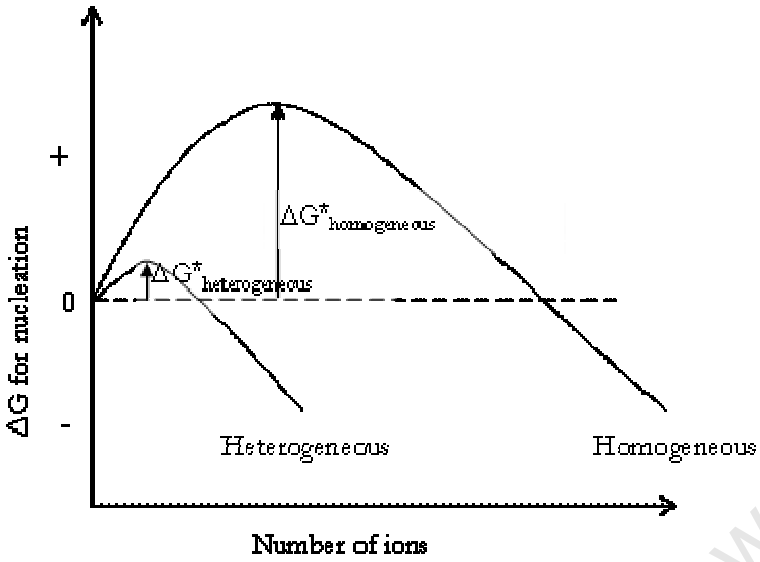

Figure 4: Effect of solid substrate to catalyse nucleation (Stumm, 1992)

2.1.3 Crystal growth

This is a process whereby the critical nucleus increases in size due to the deposition of growth units (ions or molecules) (Stumm, 1992). This process determines the final product size distribution of a process (Mullin, 1972).

2.1.4 Population balance

Particle size and distribution information is of great importance in precipitation processes. This information is given by a population balance equation and for a batch system the equation is as follows (Randolph and Larson, 1988):

$$\frac{\partial n}{\partial t} = G\frac{\partial n}{\partial L} + B - D \quad (4)$$

Where $\partial n/\partial t$ is the change in number density, $G\partial n/\partial L$ is the difference between the crystals in the interval L to L + dL, B is the birth rate and D the death rate of particles in the system as a result of nucleation, aggregation and breakage. Assuming that the particles formed are spherical in shape, a volume based histogram for the different size sub-intervals (% volume) and the particle concentration (% volume) can be used to calculate the particle number density as follows:

$$n(L)dL = \sum_i \frac{(\%\text{Volume})_i \text{ x Concentration}}{100} \text{ x } \frac{1}{k_v \overline{L^3}} \quad (5)$$

Where k_v is the shape factor and its equal to $\pi/6$

2.1.5 Scaling

When suspended/or precipitated particles from solution are deposited on equipment surfaces, they form a solid deposit referred to as scale (Sohnel and Garside, 1992). The continuous deposition of the scale on equipment surfaces can result in reduced equipment capacity and heat transfer rates (Sohnel and Garside, 1992). Hence, there is need for constant scale removal from surfaces either partially or totally in industrial set ups. This results in frequent plant shutdowns, increased maintenance costs and need for environmentally friendly waste disposal techniques. The mechanisms of scale formation can either be chemical or mechanical (Sohnel and Garside, 1992). The chemical form is supersaturation driven and occurs through either homogeneous or heterogeneous precipitation/nucleation. However, in mechanical scaling the precipitate or suspended particles are deposited on the equipment surface through weak forces of attraction (Sohnel and Garside, 1992).

Scale prevention

Chemical, mechanical and physical methods can be applied to remove scale either totally or partially (Sohnel and Garside, 1992). The chemical methods are aimed at preventing both homogeneous and heterogeneous nucleation in the system and can be achieved through

lowering the solution supersaturation level. The physical and mechanical methods involve the promotion of homogeneous nucleation and the prevention of heterogeneous nucleation respectively (Sohnel and Garside, 1992).

2.2 Adsorption

The accumulation of solutes on a surface (adsorbent), forming a film (the adsorbate) is termed adsorption (Frank, 2003). Depending on the nature of attractive forces existing between the adsorbate and the adsorbent, adsorption can be classified as either physisorption or chemisorption (Kirk Othmer, 2008). The former entails weak forces of attraction whereas the latter involves strong forces of attraction between the molecules of the adsorbate and the adsorbent. Thus, physisorption is easily reversible compared to chemisorption since less energy is required to detach the adsorbate from the adsorbent. Also, chemisorption only assumes monolayer coverage whereas in physisorption more than one layer can be adsorbed on the solid surface (Kirk Othmer, 2008).

However, applications of adsorption depend on the difference in adsorbent affinity for different components and the ability to regenerate the adsorbent (Lounici et al., 2001). Sorption is used as a general term due to the difficulties in the distinction amongst the adsorption, absorption and surface precipitation (Li and Stanforth, 2000). In order to assign the loss of solute to one of the three sorption processes, knowledge on solute and surface interaction is necessary and this can be deduced from the solute and surface properties when in solution (Stumm, 1992).

2.2.1 Adsorption isotherms

Adsorption equilibrium is often described in terms of adsorption isotherms and the commonly used isotherms being the Langmuir and Freundlich isotherm equations (Kasprzyk-Hordern, 2004). However, the fit of any data to any isotherm during surface kinetics and thermodynamics does not ascertain adsorption as the actual mechanism responsible for species removal from solution (Stumm, 1992). This is so because adsorption is mostly followed by additional interactions at the surface.

Langmuir isotherm

This isotherm was derived by Langmuir and it is based on the following assumptions (Stumm, 1992):

- Once a monolayer is formed, there is no continued deposition of the adsorbate on the adsorbent surface,
- Equal activity of adsorption sites and thus a similar mechanism of adsorbate accumulation on all adsorption sites,
- Non-interaction between adsorbed molecules.

The Langmuir equation can be expressed mathematically as follows (Ubaldini et al., 2006; Stumm, 1992):

$$q_e = \frac{q_m K_L C_e}{1 + K_L C_e} \quad \text{or} \quad \frac{1}{q_e} = \frac{1}{K_L q_m C_e} + \frac{1}{q_m}$$

$$\text{and} \quad K_L = e^{\frac{-\Delta G}{RT}} \qquad (6)$$

Where q_m - monolayer adsorption capacity (mgg^{-1}) constant

K_L - Langmuir constant (lg^{-1})

C_e - equilibrium concentration (mgl^{-1})

q_e - adsorbate adsorbed at equilibrium (mgg^{-1}).

Freundlich isotherm

This isotherm assumes an exponential decrease in the heat of adsorption as solute uptake proceeds. The Freundlich isotherm can be expressed mathematically as follows (Ubaldini et al., 2006; Stumm, 1992):

$$q_e = kC_e^{1/n} \quad (7)$$

Where k and n are constants

The two mentioned isotherms assume monolayer coverage and as result are mostly appropriate for interpreting data for chemisorption and not physisorption.

2.2.2 Adsorbents

Adsorbents must have high abrasion resistance, thermal stability and exposed surface area (Kasprzyk-Hordern, 2004). These can be classified as either polar or non-polar adsorbents. Amongst the polar adsorbents are aluminas, silica gel, and zeolites.

2.3 Alumina/aluminum oxide adsorbent

The industrial importance of aluminas (α, δ, θ, η, γ, and χ) is constantly increasing as more knowledge about them is being gathered through research (Lippens and Steggerda, 1970; Ingram Jones et al., 1996). The applications of aluminas require extensive knowledge of their properties (Kasprzyk-Hordern, 2004). According to Lippens and Steggerda (1970) aluminas can be classified as either low temperature or high temperature aluminas depending on the temperature of aluminum hydroxide dehydration. The low temperature aluminas are those obtained at dehydrating temperatures <600°C whereas the high temperature aluminas are obtained at temperatures >900°C. However, the low temperature aluminas exhibit excellent catalytic and adsorptive properties due to their high surface area and porosity (Kasprzyk-Hordern, 2004). Figure 5 below gives the sequential transformation of the hydroxides of aluminum to give the different aluminas as proposed by Lippens and Steggerda, 1970 and Ingram Jones et al., 1996.

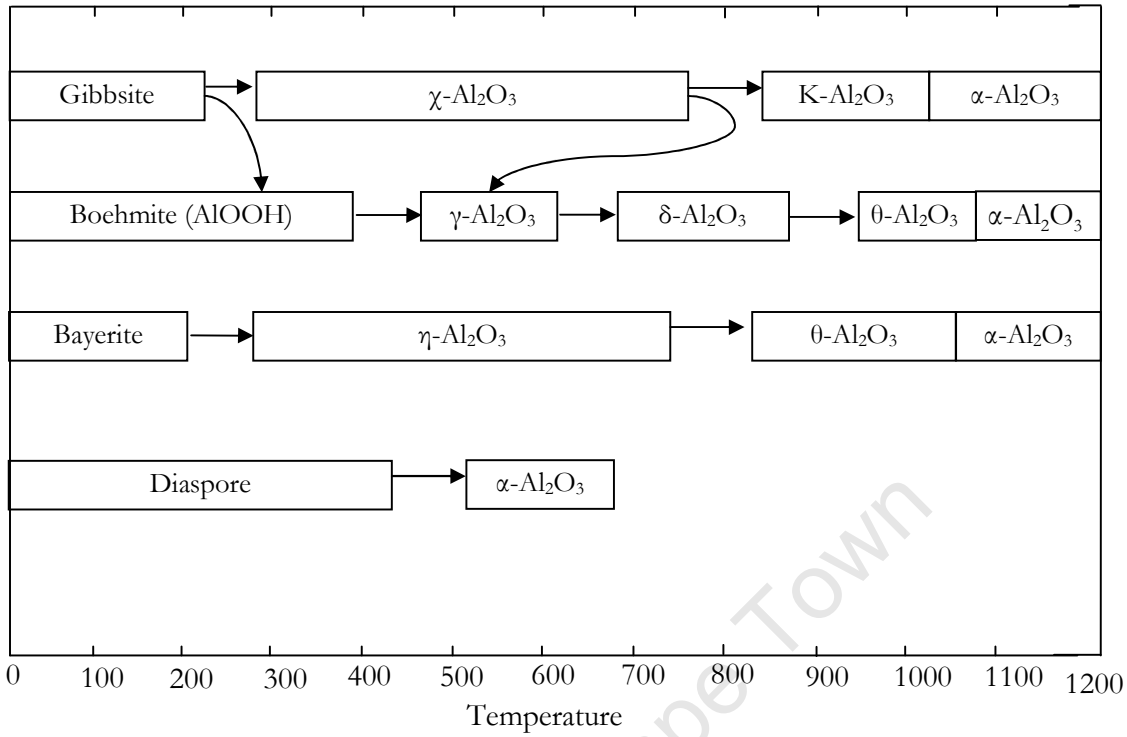

Figure 5: The thermal transitional sequence of aluminum hydroxides to aluminas (Lippens and Steggerda, 1970; Ingram-Jones et al., 1996)

2.3.1 Alumina surface properties

Mineral phases of inorganic species depending on their molecular structure and surface reactivity are susceptible to processes such as dissolution, precipitation and ion exchange when in suspension (Stumm, 1992). These processes make the mineral phases suitable for use in water treatment technology.

Activated alumina is one such mineral phase that has found wide application in industry as an adsorbent and a catalyst (Kasprzyk-Hordern, 2004; Bouguerra et al., 2007). The application of activated alumina in wastewater treatment is said to be dependent upon its oxide/aqueous interface reactions, selectivity, crystal structure, kinetics of adsorption, surface area, thermal stability and mechanical strength (Kasprzyk-Hordern, 2004). As an adsorbent activated alumina has been successfully applied in defloridation, arsenate removal, phosphate removal and desilication of wastewaters (Ghorai and Subhashini, 2005; Bouguerra et al., 2007; Lounici et al., 2001; Goldberg et al., 2002).

The reaction mechanistic, thermodynamic and kinetic properties of metal oxides in solution are influenced by the nature of their surface functional groups and the capacity of these to bind protons and adsorption ions at given pH of the solution (Goldberg et al., 2002; Stumm, 1992). Active alumina matrix can contain up to about 5% of water depending on process conditions (Kasprzyk-Hordern, 2004). Peri (1965) observed water loss even at high temperatures during alumina dehydration under a vacuum. Thus, aluminas have some water still adsorbed on their surfaces even under high temperatures.

Figure 6 shows an idealized structure of a dry and hydrated oxide surface, for example of Fe, Si and Al oxides. The idealized structure of the dry oxide illustrates the top layer to contain oxide ions over the aluminum ions. The coordinative unsaturation of the dry oxide is the driving force for the water adsorption on the surface (Stumm, 1992). Depending on temperature, water gives rise to either weak or strong binding forces of an undissociated water molecule or the dissociated form (hydroxyl group) of water molecule as shown by Figure 6 (b) and (c) respectively (Lippens and Steggerda, 1970).

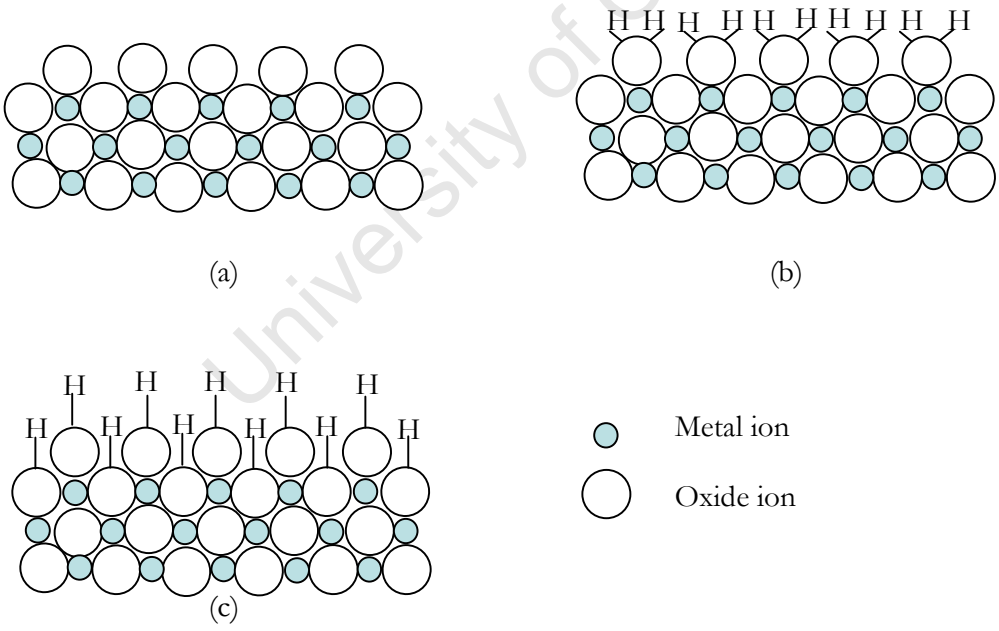

Figure 6: Idealized illustration of the cross section of the surface layer of a metal oxide (Goldberg et al., 1996; Stumm, 1992; Lippens and Steggerda, 1970).

The surface hydroxyl groups are the active sites of the activated aluminas (Goldberg, et al., 1996). Four models are being used to explain the origins of the surface hydroxyl groups namely: Peri's model, Tsyganenko's model, Knozinger's model and the Busca's model as shown in Figure 7 (a), (b), (c) and (d) (Peri, 1965; Kasprzyk-Horden, 2004). Peri's model assumes an outer layer of alumina to be only covered by Al^{vi} ions and these ions form the basis for the hydrated surface. According to Peri (1965) the good catalytic properties of γ-alumina, a low temperature alumina are due to the acid sites created during the dehydration process.

Tsyganenko's model suggests that the number of Al atoms attached to the OH group is the determining factor on the frequency of hydroxyl groups. On the other hand, Knozinger's model states that the net electrical charge on the OH group is the one which determines the frequency of the hydroxyl groups. Busca's model suggests the presence of cation vacancies as the determining factor on the frequency of the hydroxyl groups on aluminas (Kasprzyk-Horden, 2004). Morterra and Magnacca (1996) reported a difference in the OH spectrum of transition aluminas and the aluminum hydrated phases. The spectra for the activated aluminas are almost the same though minor differences on intensities can be observed at times.

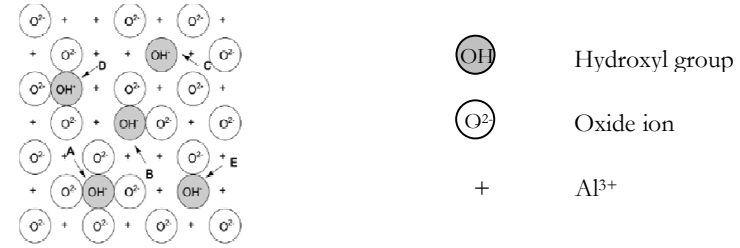

(a)

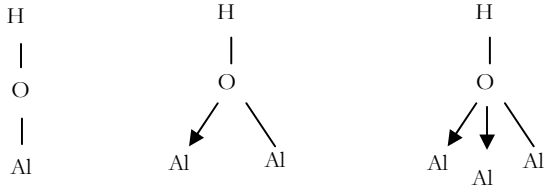

(b)

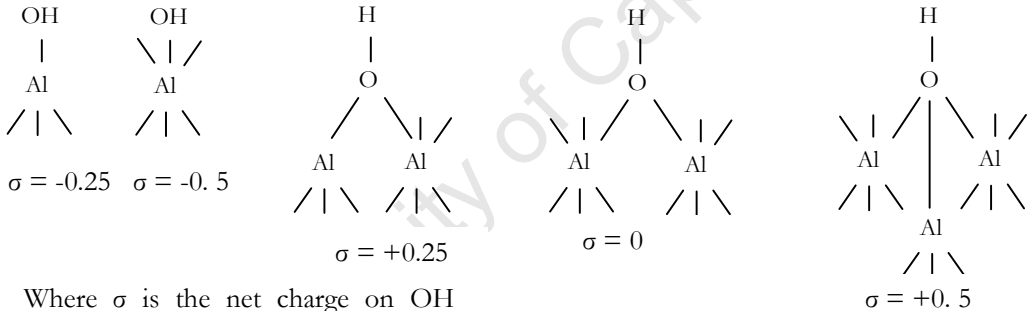

(c)

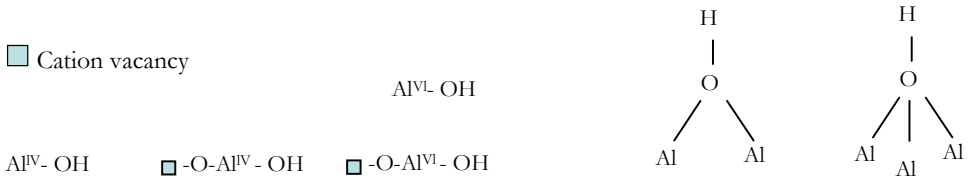

(d)

Figure 7: Possible surface hydroxyl groups on aluminas (Peri, 1965; Kasprzyk-Horden, 2004)

The surface hydroxyl groups can therefore be idealized as those coordinated with one aluminum ion, two aluminum ions and those coordinated by three aluminum ions. The reactivity of alumina surfaces is as a result of these hydroxyl groups which render them amphoteric (possessing the acid–base properties) (Goldberg et al., 1996; Riemsdijk et al., 1986).

2.3.2 Chemistry of alumina in aqueous systems

The chemistry of activated aluminas in solution is of importance when studying its applications industrially (Goldberg et al., 1996). The origins of alumina reactive surface groups are believed to be as a result of its reactions with water. These groups arise as a result of alumina dissolution, precipitation and superficial hydration (Carrier et al., 2007; Vogelsberger et al., 2008). For pH greater than 4, Carrier et al., (2007) found out that when γ-alumina is in solution it undergoes dissolution which leads to supersaturation of the system with respect to aluminum hydroxides which results in subsequent precipitation of the hydroxide/hydrated phases. They also accredited the difficulty in the reproducibility of alumina chemistry findings to the strong dependence of the nature and heterogeneity of the hydroxides formed on experimental conditions such as pH, time, and temperature. Another very important finding was that of the particle size having an effect on the kinetics of alumina dissolution (Roelofs and Vogelsberger, 2006; Vogelsberger et al., 2008). The dissolution for the nanoparticles of alumina gave a maximum at the beginning of the experiment which decreases and equilibrates with time. The analysis of the precipitated solids using X-ray diffraction analysis showed that bayerite was formed when the alumina is in solution for pH greater than 4.5. They also suggested that the alumina hydration is most likely not limited to the oxide/water interface.

The dissolution kinetics of alumina is controlled by the concentration of charged surface groups (Stumm, 1992). For a system consisting of pure water and alumina particles, these charged surface groups can be attributed to the ionisation reactions happening on the hydrated alumina surface as shown by equations 8 and 9 (Goldberg et al., 1996):

$$AlOH + H^{+} \leftrightarrow AlOH_2^{+} \quad (8)$$

$$AlOH \leftrightarrow AlO^{-} + H^{+} \quad (9)$$

Equations 8 and 9 depict the amphoteric nature of the surface hydroxyl groups, which constitute the reactive sites of the alumina surfaces. In addition, Equation 8 and 9 show how an alumina surface develops an electrical charge as a result of the ionisation of the surface groups. Thus, the surface charge is due to the loss of ions and the adsorption of charged species (anions and cations) (Kasprzyk-Horden, 2004; Stumm and Morgan, 1981). Oxoanions are said to form either bimolecular or multimolecular surface complexes with oxides (Kasprzyk-Horden, 2004). This charge/potential as a result of gaining or releasing an ion is called the zeta potential and is dependent on the pH of the solution (www.malvern.co.uk). The point of zero charge (pzc), which is the point of colloidal least stability, is of importance for practical applications of oxides. Many researchers report the point of zero charge for alumina to be typically between a pH of 7 and 10 depending on the type of alumina (Kasprzyk-Hordern, 2004; Goldberg et al., 1996; Yopps and Fuerstenau, 1964). Depending on the alumina charge, an equal amount of opposite ion charge must be adsorbed on to the alumina surface in order to maintain electrical neutrality (Goldberg, et al., 1996). Low zeta potential values of particles results in dispersion instability as there is no force to prevent particle-particle interaction (www.malvern.co.uk). In contrast to other studies, Kosmulski et al., (2009) reported the alumina zeta potential being not sensitive to pH, the nature and concentration of the salt. However, he found out that activated alumina preferentially adsorbs sulphate to magnesium. Figure 8 below shows the dependence of surface charge of alumina on pH.

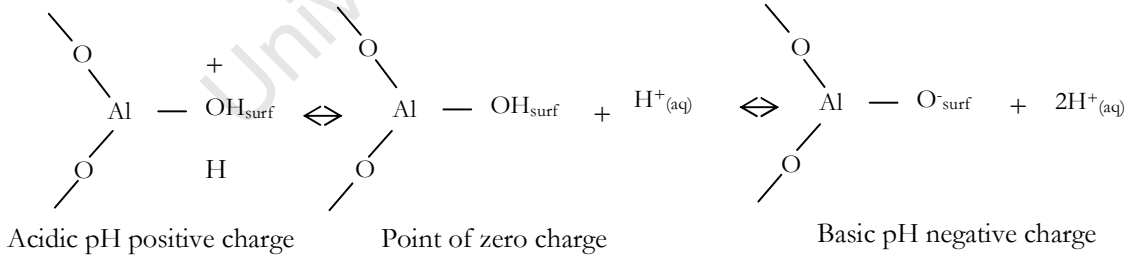

Figure 8: Surface charge of alumina as a function of medium pH (Kasprzyk-Hordern, 2004)

From Figure 8, the ionisation of the surface renders it susceptible to surface reactions in order to preserve electrical neutrality. Activated alumina is reported to be a good adsorbent for silicon species at alkaline conditions (Matson, 1981) despite silica being negatively charged for pH greater than 4 (Kosmulski, 2006). Studies by Bouguerra et al., (2007) on the

kinetics of silica adsorption onto activated alumina showed high silica removals at pH 8.0 to 8.5. This high silica removal at basic pH, despite the surfaces of both alumina and silica negatively charged must be as a result of the chemistry of the two species when in solution.

2.4 Silicon and aluminum

Both silicon and aluminum normally exist as compounds bonded with other species especially oxides (Stumm and Morgan, 1996). Silica is silicon bound to oxygen and this is the most abundant compound of silicon. When in solution aluminum and silicon in the form of silica both undergo hydration (Iler, 1979; Stumm and Morgan, 1996).

2.4.1 Dissolution of silica in solution

Silica exists in three different forms: reactive (dissolved silica), colloidal (polymeric form) and suspended particles (Peairs, 2007; Sheikholeslami and Tan, 1999, Iler, 1979). In the solid phase, silicon exists as either crystalline or amorphous silica. Crystalline silica has low solubility compared to amorphous silica in water at 25°C (Iler, 1979).

Silica solubility is reported to be a function of pH, the presence of other species, temperature and pressure (Fournier and Rowe, 1977; Sheikholeslami et al., 2001; Chen et al., 1982; Iler, 1979; Owen, 1972;). The removal of silicon species from waste-waters is fundamentally dependent on its form (Iler, 1979). The reactive form being the silicon dioxide (SiO_2) dissolved in water to form the monomeric form (H_4SiO_4) (Iler, 1979). At a temperature of 25°C and concentrations less than 2 x 10^{-3} M, silica remains in the monomeric form over long periods. However, when the concentration is increased it polymerises to form colloids (Iler, 1979). The reactive form of silica ionises under alkaline conditions and the degree of ionisation increases with an increase in pH (Peairs, 2007). The dissolution of amorphous SiO_2 to give the different silicon species in solution and the solubility constants is given by the following equilibrium equations extracted from Stumm and Morgan, 1996:

$$SiO_2 + 2H_2O \leftrightarrow H_2SiO_4 \qquad \log K = -2.7 \qquad (10)$$

$$Si(OH)_4 \leftrightarrow H_3SiO_4^- + H^+ \qquad \log K = -9.46 \qquad (11)$$

$$H_3SiO_4^- \leftrightarrow H_2SiO_4^{2-} + H^+ \qquad \log K = -12.56 \qquad (12)$$

$$4Si(OH)_4 \leftrightarrow H_6Si_4O_{12}^{2-} + 2H^+ + 4H_2O \qquad \log K = -12.57 \qquad (13)$$

The total concentration of dissolved silica in solution at any given pH is given by the sum of the concentration of the solubilised silica species as follows:

$$[Si_T] = [Si(OH)_4] + [H_3SiO_4^-] + [H_2SiO_4^{2-}] + [H_6Si_4O_{12}^{2-}] \qquad (14)$$

The relative concentrations of silica species at equilibrium with amorphous silica during dissolution at 25°C for the entire pH can be computed using the equilibrium data from the above equations 10-13. Thus the relative concentration of silica in solution at equilibrium with amorphous silica at any given pH is given by the following equations (Stumm and Morgan, 1996):

$$\log [Si(OH)_4] = -2.7 \qquad (15)$$

$$\log [H_3SiO_4^-] = -12.16 + pH \qquad (16)$$

$$\log [H_2SiO_4^{2-}] = -24.72 + 2pH \qquad (17)$$

$$\log [H_6Si_4O_{12}^{2-}] = -23.37 + 2pH \qquad (18)$$

The amount of silica species at equilibrium with amorphous silica as a function of pH is given by Figure 9.

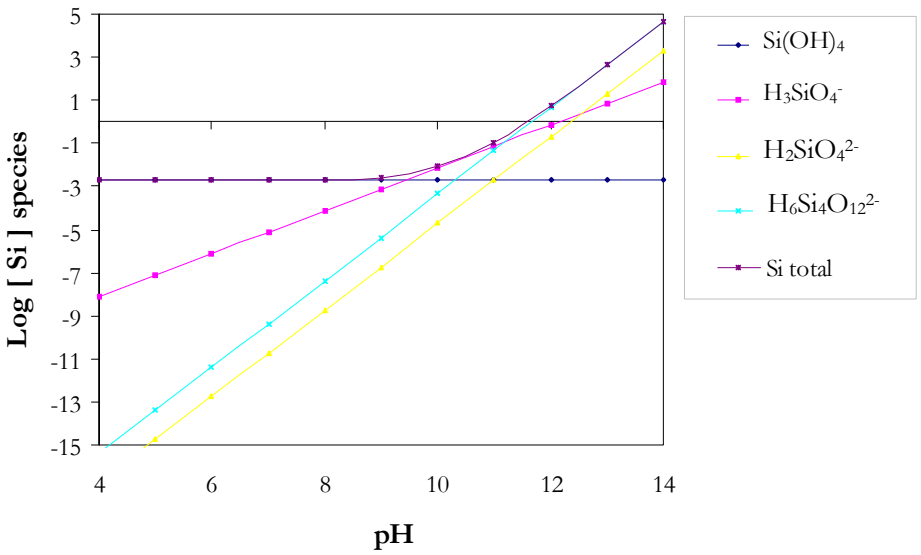

Figure 9: Solubility-pH diagram for amorphous silica dissolution at 25°C and Ionic strength = 0.5.

2.4.2 Hydrolysis of Al (III) in solution

Aluminium undergoes hydrolysis to the different hydroxyl complexes as a function of solution pH (Stumm and Morgan, 1986). Depending on solution pH, aluminum can exist as either the monomeric or polymeric form. The monomers are dominant at pH values around pH 7 whereas the polymers are dominant at higher pH values (Berkowitz et al., 2005). Aluminum speciation is very important for its removal from wastewaters. The equilibria constants governing the formation of these aluminum complexes from gibbsite ($Al(OH)_3$) at 25°C are given by equations 19-24 as in Stumm and Morgan, 1996.

$$Al^{3+} + H_2O \leftrightarrow Al(OH)^{2+} + H^+ \qquad \log K = 3.53 \qquad (19)$$

$$Al^{3+} + 2H_2O \leftrightarrow Al(OH)_2^+ + 2H^+ \qquad \log K = -0.8 \qquad (20)$$

$$Al^{3+} + 3H_2O \leftrightarrow Al(OH)_3 + 3H^+ \qquad \log K = -6.5 \qquad (21)$$

$$Al^{3+} + 4H_2O \leftrightarrow Al(OH)_4^- + 4H^+ \qquad \log K = -14.5 \qquad (22)$$

$$3Al^{3+} + 4H_2O \leftrightarrow Al_3(OH)_4^{5+} + 4H^+ \qquad \log K = 11.6 \qquad (23)$$

$$13Al^{3+} + 28H_2O \leftrightarrow Al_{13}O_4(OH)_{24}^{7+} + 32H^+ \qquad \log K = 11.8 \qquad (24)$$

The total concentration of Al^{3+} in solution at any given pH is given by the sum of the concentration of the different Al hydroxyl complexes as follows:

$$[Al_T] = [Al^{3+}] + [Al(OH)^{2+}] + [Al(OH)_2^+] + [Al(OH)_3] + [Al(OH)_4^-] + [Al(OH)_4^{5+}] + [Al_3O_4(OH)_{24}^{7+}] \qquad (25)$$

The combination of the solubility product of gibbsite and the complex formation constants can be used to compute the concentrations of the different Al species in solution at 25°C and at any pH. Equations 26-32 give the relationship between the concentrations of Al^{3+} species and pH as obtained from Stumm and Morgan, 1996. The plot of these equations is given by Figure 10.

$$\log[Al^{3+}] = 8.5 - 3pH \qquad (26)$$

$$\log[Al(OH)^{2+}] = 3.5 - 2pH \qquad (27)$$

$$\log[Al(OH)_2^+] = -0.8 - 2pH \qquad (28)$$

$$\log[Al(OH)_3] = -6.5 \qquad (29)$$

$$\log[Al(OH)_4^-] = -14.5 + pH \qquad (30)$$

$$\log[Al(OH)_4^{5+}] = 11.6 - 5pH \quad (31)$$

$$\log[Al_3O_4(OH)_{24}^{7+}] = 11.8 - 7pH \quad (32)$$

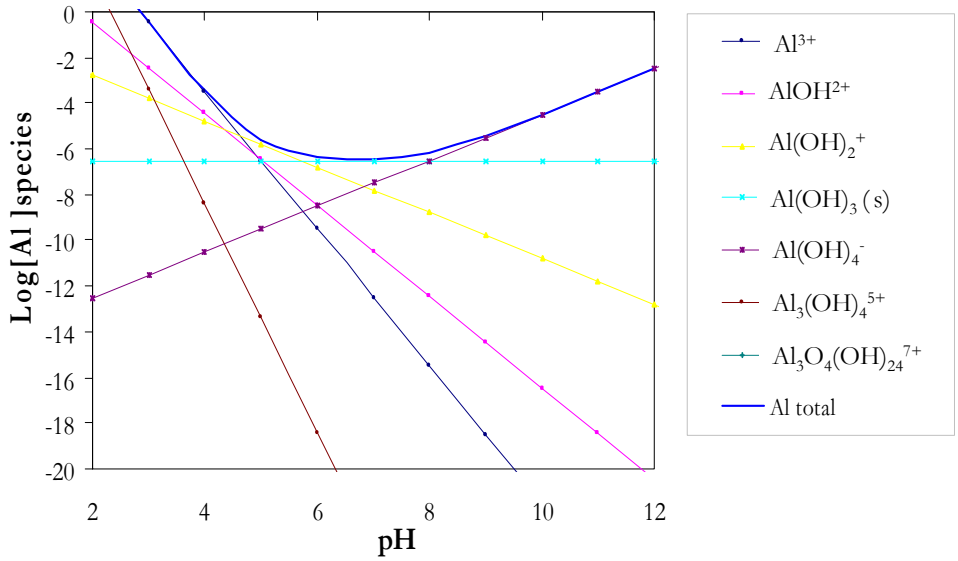

Figure 10: Solubility-pH diagram of amorphous aluminium hydroxide hydrolysis at 25°C (Stumm and Morgan, 1996)

2.5 Possible removal mechanisms of silicon species by alumina in solution

Numerous methods of treatment and removal of silicon species from wastewaters have been an area of great interest to many researchers (Bremere et al. 2000; Matjie and Engelbrecht, 2007; Sheikholeslami et al., 2001). Most of these methods employed are generally specific to brine composition and process conditions. Activated alumina application in silicon species removal in waste-waters is an area of great interest to many researchers though the mechanism of silica removal is still a non unified concept (Midkiff, 2002; Bouguerra et al. 2007; Matjie and Engelbrecht, 2007).

Many researchers have reported the unique affinity between silica and aluminum oxides (Birchall, 1994: Houston et al. 2008). Mostly, they accredit the affinity to the similar configuration of both silica and aluminum oxides when in solution (Birchall, 1994; Doucet et

al., 2001; Hanzlicek and Steinerova-Vondrakova, 2002). In the presence of silica and aluminum in solution, hydroxyaluminosilicates (HAS) are reported to form though the mechanism of formation is not fully understood (Doucet et al., 2001). Doucet and co-workers (2001), concluded that the formation of HAS was as a result of competitive condensation of silicic acid on the hydroxylated alumina surface. Also, they noted that silicon species continued to be deposited on the surface when silica is in excess.

Exley and Birchall (1992) in their studies of HAS formation, concluded that the mechanism of formation proceed through the inhibition of the nucleation of aluminum hydroxide. They also concluded that the silicic acid substituted hydroxylated aluminum at growth sites on aluminum hydroxide matrix and this was dependent upon solution pH and the silicic acid concentration.

Under alkaline conditions silica co-exists as both the colloidal and soluble form (Iler, 1979). Considering that under alkaline conditions, alumina undergoes transformation, dissolution and subsequent precipitation when in solution resulting in the formation of the surface hydroxyl groups, the removal mechanism(s) of silicon species by alumina can be as a result of the following:

i. Adsorption onto the hydrated alumina/newly precipitated hydroxides which is then followed by surface precipitation (Iler, 1979; Li and Stanforth, 2000; Doucet et al., 2001).
ii. Precipitation with the insoluble metal hydroxides and solubilised Al ions

2.5.1 Adsorption and surface precipitation

Surface precipitation is the continued deposition of species on the already deposited one on the mineral surfaces (Li and Stanforth, 2000). Li and Stanforth (2000) studied the removal of phosphate by goethite. They concluded that the removal of phosphate by goethite was by adsorption which was then followed by surface precipitation. Once a film of phosphate was deposited on the goethite surface, the adsorption sites were obscured and the continued removal of phosphate was due to a different reaction mechanism from adsorption (surface precipitation). However, the complication is in determining the point of transition from adsorption to surface precipitation. Li and Stanforth (2000) and Tejedor-Tejedor and

Anderson (1990) suggested the use of change in zeta potential to distinguish the transition from adsorption to surface precipitation. The size of the charge on the surface varies linearly with surface coverage for adsorption.

Many researchers report the removal of dissolved silica by alumina in solution to be a result of the dissolved silica ($Si(OH)_4$) condensing with the OH groups of the hydrated alumina surface (Hanzlicek and Steinerova-Vondrakova, 2002: Doucet et al., 2001) . This deposition of the reactive silica is said to increase the surface area as further deposition occurs on silica to form a film of silica as shown below in Figure 11(Iler, 1979; Hanzlicek and Steinerova-Vondrakova (2002)):

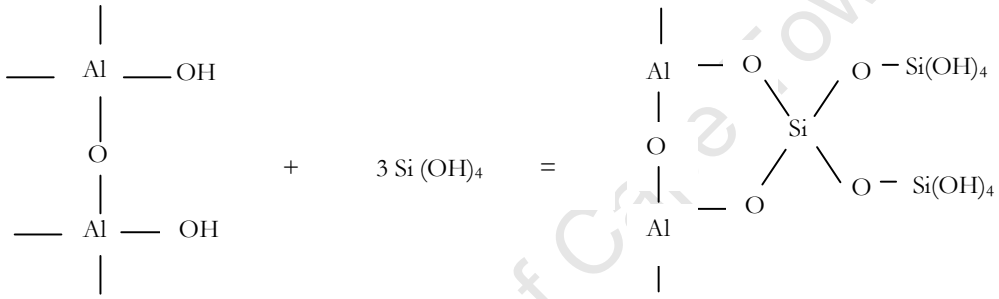

Figure 11: Interaction of silica and alumina resulting in an increase in surface area for further deposition of silica

Selim et al. (1996) observed a shift in silica spectra during silica removal by alumina. They accredited the shift to the formation of a surface complex. Iler (1979) reviewed the formation of quartz in a suspension of iron and aluminum hydroxides at 20°C, at dilute concentrations of iron, aluminum and silica. However, there was no quartz precipitation observed from a saturated solution of amorphous silica containing high concentrations of monomeric silica (Iler, 1979). In review Iler (1979) also stated the reduction of silica equilibrium solubility to below 9.5ppm in the presence of trace amounts of alumina or iron at 20°C. Also at pH 7.0 to 9.0 when silica concentration exceeded 6mg/l, mineral quartz was reported to have precipitated out (Drever, 1988).

2.5.2 Precipitation with the insoluble metal hydroxides and solubilised Al ions

When metal oxides undergo dissolution this brings about hydrolysis, formation of metal oxide precipitates and silica adsorption onto the precipitate (polymerisation) (Iler, 1979). Also, in the presence of dissolved aluminum and other species, silica has a tendency of forming aluminosilicates (Gabelich et al., 2005). The different aluminosilicates are not only made up of silica and aluminum but have other elements bound within the matrix (Gallup et al., 2003) due to the complexity of natural waters and waste-waters. The complexity of industrial waste-waters and natural waters has also led to the study of the effects of the presence of other species on the removal of silica. Amongst the studies was the effect of cations and competing anions on silica removal and boron removal (Manning and Goldberg, 1996; Goldberg et al., 1996; Bouguerra et al., 2007; Bouguerra et al., 2008; Chen et al., 1982)

Bouguerra et al., (2008) showed that the adsorption of boron onto alumina decreases in the presence of anions such as silica, nitrate and hydrogenocarbonate. However, the adsorption of silica onto alumina was not affected by the presence of foreign particles such as sulphate, fluoride, nitrate and hydrogenocarbonate (Bouguerra et al., 2007). This shows the unique affinity of alumina for silica.

Sheikholeslami and Tan (1999) in their study of silica removal from solutions reported the catalysis of silica polymerization by calcium and magnesium salts. According to Chida et al., (2007) polysilicic acid is stable in solution in the presence of calcium ions. Bremere et al., (2000) also found out that the addition of iron (III) in solution enhances silica monomer deposition from solution. Iler (1979) reviewed the optimum removal of soluble silica by aluminum ions at pH of 8 to 9. Under acidic conditions 1 part Al^{3+} was found to be needed to precipitate out 40 parts of colloidal silica. However, under alkaline conditions at least 4 parts Al^{3+} are required to remove 1 part soluble silica (Okamoto et al., 1957).

According to Stumm and Morgan (1981), the mechanism by which aluminol groups (as a result of hydration) on alumina surfaces removes ions from solution is by either inner-sphere or outer sphere complexes. This is dependent on system pH, ion concentrations and suspension density of the adsorbent. At very low concentrations adsorption of metal ions can be considered as a bimolecular adsorption reaction (Goldberg et al., 1996). For divalent

Me^{2+} ions, Equations 33-35 illustrate the possible mechanisms by which the metal ions can react with the hydroxyl groups (Janusz et al., 2003; Huang and Stumm, 1973; Hohl and Stumm, 1976):

$$AlOH + Me^{2+} + H_2O \rightarrow AlOMeOH + 2H^+ \quad (33)$$

$$2AlOH + Me^{2+} \rightarrow AlO-Me-OAl + 2H^+ \quad (34)$$

$$AlOH + Me^{2+} \rightarrow AlOMe^+ + H^+ \quad (35)$$

Huang and Stumm (1973) found that the extent of alkaline earth cations uptake by hydrous gamma alumina increases with an increase in pH and also as one goes down the group. The authors above also found out that finite adsorption occurs at the point of zero charge and pH values slightly below the point of zero charge. Houston et al. (2008) in their studies on aluminum removal by silica concluded that the removal mechanism involves Al sorption to silanol sites, surface enhanced precipitation of the hydroxide and bulk precipitation of an aluminosilicate. Houston et al., (2008) also concluded that cations such as Na^+ acted as a charge compensating ions. Since both silica and alumina have an isostructure (Birchall, 1994), one can conclude that they interchange reactions.

2.5.3 Possible formation of aluminosilicates

The existence of both dissolved aluminum and silica in solution can result in the formation of aluminosilicates. Drever (1988) found out that at aluminum concentrations of 10^{-7} M and silica concentrations of 10^{-4} M, the wastewater under investigation was supersaturated with respect to kaolinite and gibbsite. Jardine and co-workers (1985) reported the uptake of the monomeric and polymeric form of aluminum by aluminosilicates such as kaolinite and montmorillonite. The following equations show some of the reactions in a multivalent ionic system containing silica, calcium and aluminum (Matjie and Engelbrecht, 2007):

$$2Al^{3+} + 2H_4SiO_4 + H_2O \rightarrow Al_2Si_2O_5(OH)_4 + 6H^+ \quad (36)$$

$$3Ca^{2+} + 6Al(OH)_4^- + 12OH^- \leftrightarrow 3CaO.Al_2O_3.6H_2O \quad (37)$$

2.6 Recovery of alumina loading capacity through dissolution of the aluminum silicate species

The economic viability of using adsorption in waste-water treatment is to a large extent dependent on the capability of regenerating the adsorbent bed. A regeneration method with higher adsorption capacity recovery renders adsorption an attractive and effective waste water treatment technique. The regeneration technique used depends on the adsorbate chemical form and the intermolecular interaction between the adsorbate and the adsorbent (Lounici et al., 2001). As a result, saturated alumina bed can be regenerated either chemical or electrical. Also, at times both chemical and electrical regeneration can be implemented in conjunction depending on the form of the adsorbates.

The regeneration of an alumina bed saturated by fluoride showed that using a combination of electro-regeneration and chemical regeneration gave the best results (Lounici et al., 2001). Sodium hydroxide and sulphuric acid are amongst the different reagents used (Lounici et al., 2001).

Regeneration of alumina saturated with aluminosilicates would involve the dissolution of the aluminosilicates to the bulk solution. Aluminosilicate dissolution involves the breaking of the Si-O and Al-O bonds (Oelkers and Schott, 1995). Thus, water, acids, ligands and hydroxides can be used to facilitate aluminosilicates dissolution (Cama et al., 2002: Oelkers and Schott, 1995). In ligand promoted dissolution, the dissolution rate is promoted if the ligand uptake forms monomolecular inner-sphere complexes and not binuclear and multinuclear surface complexes (Kasprzyk-Horden, 2004).

Under alkaline conditions the binding of an additional OH group in the surface complex or the deprotonation of a surface OH facilitates dissolution (Sheikholeslami et al., 2001). Previous studies have shown that silicates dissolution under alkaline conditions depend on the surface concentration of silica (Stumm, 1997). The dissolution rates of kaolinite were found to increase with temperature and decrease with pH (Cama et al., 2002). Anorthite dissolution under acidic conditions can be expressed as follows (Oelkers and Schott, 1995):

$$CaAl_2Si_2O_8 + 8H^+ \leftrightarrow Ca^{2+} + 2Al^{3+} + 2SiO_2(aq) + 4H_2O \quad (38)$$

From the above equilibrium equation, introduction of an alkali will shift the equilibrium to the left. Also, the dissolution rates of oxides and silicates was found to increase with decreasing pH below their pH of point of zero charge and increase with increasing pH in the alkaline region due to surface ionisation (Stumm, 1997; Kasprzyk-Horden, 2004). Hellmann (1995) also noted the preferential dissolution of Al and Si to be a function of the element speciation at the given pH conditions. The Al dissolution is preferential under acidic to neutral pH conditions and greatest at extreme basic conditions. This is due to the dominance of the protonated hydroxylated alumina group with respect to the neutral silica at acidic to neutral pH and the co-existence of deprotonated hydroxylated silica and alumina groups. Oelkers and Schott, (1995) in their studies also concluded that the number of the different types of bonds to be broken as well as their relative strength and reactivity accounts for the difference in dissolution equilibrium. This was further confirmed by Pelmenschikov et al. (2001) studies on dissolution of silica surfaces. Pelmenschikov et al., (2001) established that the calculated energy barrier for silica hydrolysis is higher than the activation energy of silica dissolution at neutral silica surfaces. In explanation to this discrepancy, they proposed that the Si-O-Si bond hydrolysis is followed by its dehydroxylation. Thus, the rate of dissolution is proportional to the concentration of surface bound OH, the extent of surface deprotonation/protonation, the concentration of adsorbate, compounds or elemental speciation, the number of the different types of bonds and their relative reactivity and the nature of alkali cations (Sheikholeslami et al., 2001; Hellman, 1995; Stumm, 1997). Theoretically, the formation of a surface precipitate on solid/water interface is expected to introduce a dissolution barrier to the release of species into solution. However, Hellman (1995) studies in aluminosilicates dissolution showed that the effect caused by surface precipitates was negligible. The interconnected porosity of precipitates and the leached layer depths were stated as the main reasons for the uncharacteristic behaviour. An increase in leaching depth increases the number of Al-O and Si-O bonds susceptible to hydrolysis (Hellmann, 1995). In general, dissolution can be either transport controlled or surface controlled (Stumm and Morgan, 1996).

3 MATERIALS AND METHODS

3.1 Analytical techniques

Chemical analysis of solutions

The chemical analyses of the solutions were done using Atomic Absorption Spectroscopy (AAS) and the Inductively Coupled Plasma-Atomic Emission Spectroscopy (ICP-AES) for the determination of concentrations of aluminium, calcium and silicon species. Prior to analysis the samples were filtered through 0.2μm Millipore cellulose acetate filters in order to remove suspended solids or precipitates. For repeatability, samples were taken in duplicate. The pH values of solutions were measured with a Hanna pH 211 meter.

Chemical analysis of solids

The purity and morphology of the solid activated alumina were determined using the X-Ray Diffraction (XRD) and the Scanning Electron Microscope (SEM) respectively. The particle size evolution was carried out using the Malvern mastersizer and the micro electrophoretic zeta potential analyzer for the particle size distribution. The micro-electrophoretic zeta potential analyzer was also used to measure the alumina zeta potentials.

3.2 Materials and chemicals

The following analytical grade Merck chemicals were used during the experiments: 98% calcium sulphate dihydrate ($CaSO_4.2H_2O$), sodium metasilicate pentahydrate ($Na_2SiO_3.5H_2O$), 99% aluminium sulphate ($Al_2SO_4.18H_2O$), 98% sodium gluconate, 99% silicon dioxide, 99% sulphuric acid and 98% sodium hydroxide. The adsorbent material used was activated alumina.

The pH for the different samples of the gas condensate was found to be between 8.3 and 9.6. The synthetic solutions used to simulate the gas liquor were prepared from the hydrated salts: calcium sulphate hydrate ($CaSO_4.2H_2O$), sodium metasilicate pentahydrate ($Na_2SiO_3.5H_2O$), aluminium sulphate hydrate ($Al_2SO_4.18H_2O$). Hydrated salts were used because of their ease to dissolve compared to anhydrous salts. The synthetic solutions were prepared by dissolving these salts in deionised water and then adjusting the pH to between

8.3 and 9.0. Magnetic stirrers were used for agitation during synthetic solutions preparation. The synthetic solution concentration with respect to each scaling species was modelled on that of the raw gas condensate as shown in Table 1.

Table 1: The desired theoretical concentrations of the synthetic solutions with respect to each aluminum silicate species

Element	Solution concentration (ppm)
Si	10.0
Al	5.0
Ca	5.0
Fe	2.0

3.3 Experimental Design

Batch mode experiments

Batch experiments for the activated alumina loading and unloading were conducted in 2 litre (l) beakers. During these experiments, the gas condensate and the synthetic solutions pH were adjusted to the desired pH values of 8.3 to 9.0. Activated alumina loading experiments by the gas condensate were carried out either at room temperature or 40°C±1°C and at a minimum alumina dosage of 25g/l. The desired pH was maintained by either using sulphuric acid or sodium hydroxide as titrants whilst the temperature was controlled by immersing the reaction vessels in a thermostatically controlled water bath.

Continuous mode experiments

The continuous loading experiments were conducted in a jacketed, packed bed column at the gas condensate pH (8.3 to 9.0), a temperature of 40°C±1°C, a minimum residence time of 6 minutes and an activated alumina dosage of not less than 25g/l. The gas condensate feed was pumped into the column at a fixed flow rate until equilibrium was reached. The equilibrium point for these experiments was taken as the point when there was no detectable change in the level of contaminant removal as measured by ICP-AES. The gas condensate contaminant removal was measured as a function of time and/or cumulative volume by

analysing the effluent's species concentrations using ICP-AES. On the other hand, the continuous regeneration/or unloading experiments were conducted in a jacketed column at room temperature and minimum residence time of 3 minutes. Sulphuric acid and sodium hydroxide cleaning reagents were pumped into the column at a fixed flow rate until equilibrium was attained.

For both batch and continuous experiments the time required for reaching equilibrium was determined by removing samples at regular time intervals. The samples were filtered through a 0.2μm Millipore cellulose acetate filter and the filtrate analysed for the Al, Si and Ca species (aluminosilicate species) concentrations using ICP-AES and AAS. A schematic diagram of the experimental apparatus for the continuous experiments is as shown in Figure 12. The contaminant percentage removal for the individual metal ions was calculated as follows:

$$\%\ \text{Species removal} = \frac{\left(C_{\text{initial}} - C_{\text{final}}\right)}{C_{\text{initial}}} \times 100 \tag{39}$$

Where $C_{initial}$ and C_{final} are the initial and the final concentrations (mg/l) of the individual element.

Likewise, the percentage species unloaded from the spent alumina was calculated as follows:

$$\%\ \text{Species unloaded} = \frac{\text{Mass in effluent}}{\text{Mass initial adsorbed}} \times 100 \tag{40}$$

The mass initially loaded onto alumina was determined from the loading curves and the overall mass balance for the loading experiment.

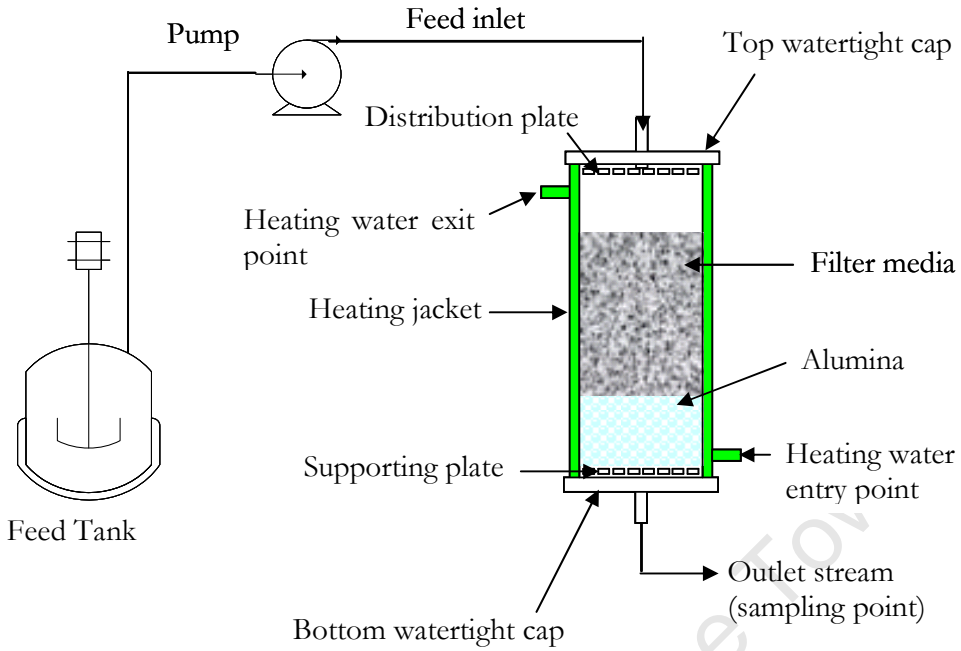

Figure 12: Schematic diagram of the experimental system used for the continuous mode experiments.

3.4 Experimental program

The experiments were carried out in three phases as follows:

1. Investigation into the activated alumina chemistry in solution;
2. Understanding the mechanisms of aluminum silicate species removal by activated alumina;
3. Investigation into the unloading of the loaded bed of activated alumina by the aluminum silicate species.

3.4.1 Investigation into alumina surface chemistry in solution

Under this phase, the following experiments were conducted:

- Investigation into the dissolution and transformation behaviour of alumina when in suspension;

- Determination of activated alumina and silica zeta potential.

Dissolution and transformation behaviour of alumina when in suspension

The investigations into activated alumina transformation and dissolution when in suspension were conducted batch-wise. For these experiments, alumina to water/gas condensate ratio of 1g/80ml and 1g/40ml was used. The activated alumina pellets were ground using a pestle and mortar. The fine particles used from sieving were in the size range of 25μm<d<75μm. One batch of experiments was carried out using activated alumina pellets and the other with the ground activated alumina. In order to compare and relate the fines experiment to the mechanism for the species removal, alumina pellets were washed to give the nanosized particles. The nanoparticles were also investigated for the dissolution properties and the particle size evolution. A pitch blade impeller was used to minimize particle breakage and settling of the particles. A pH range of 8.3 to 9.0 was maintained. 0.1M NaOH and 0.1M HCl were used to adjust the pH throughout the experiment. Liquid samples were collected at short intervals for a total aluminium analysis by an AAS and ICP-AES. The particle size distribution within the suspensions as a function of time was also investigated using a micro-electrophoretic zeta potential analyzer and the Malvern mastersizer for the activated alumina fine particle experiments. The experiments were aged up to 6 days. The fines and pellets were oven dried at 60°C and analysed for their structural properties using XRD.

Zeta potential measurements

A micro electrophoretic zeta potential analyzer was used to measure the zeta potential of activated alumina and silica as a function of pH. The activated alumina and silica were ground into a fine powder and filtered through a 1μm filter as the analytical instrument required that the particle size be ≤6μm. Furthermore, in order to assist the filtration process, the sample container was placed in an ultrasonic bath. In order to establish the dependence of zeta potential on pH, the suspension was continuously stirred using a magnetic stirrer and the pH was varied using standard solutions of 0.1M HCl and 0.1M NaOH. The zeta potential was used to infer the most likely reactions which alumina and silica can undergo at the experimental conditions under investigation.

3.4.2 Understanding the mechanisms of aluminum silicate species removal by alumina

The experiments to investigate the mechanism of species removal by activated alumina were carried out batch wise. Gas condensate and the synthetic solutions were used. 25g of both fines and pellets of activated alumina were suspended in 1000ml of both the gas condensate and the synthetic solutions. The experiments were carried out at room temperature and 40°C±1ºC and a pH range of 8.3 to 9.0. Liquid samples were collected and filtered through a 0.2μm filter for species analyses with AAS and ICP-AES at regular short intervals. The evolution of the aluminum silicate species and the activated alumina surface chemistry results were analysed to explain the possible mechanism of species removal. The mechanism of species removal was also inferred from the evolution of the aluminosilicate species in the gas condensate during continuous loading of activated alumina at a temperature of 40°C±1ºC and activated alumina dosage of at least 25g/l.

3.4.3 Investigation into the unloading of the loaded bed of alumina

The experiments to investigate the possibility of regenerating activated alumina were conducted batch-wise and continuously. Gas condensate was continuously fed through a jacketed, packed bed column with an alumina dosage of at least 25g/l, operated at a temperature of 40ºC±1ºC with a residence time of 6 minutes in order to load the activated alumina with the aluminum silicate species. The contaminant removal was measured over time by analyzing for the aluminum silicate species concentrations in the effluent stream.

Once loaded, the unloading of the activated alumina was carried out batch-wise and continuously at room temperature. NaOH (aq), H_2SO_4 (aq) and sodium gluconate solutions of varying concentrations were used. An alumina to wash reagent ratio of 1g to 40ml was used. The regeneration time was 2 hours. The aluminum silicate scaling species concentrations were determined at regular intervals and hence the percentage (%) unloading of the aluminum silicate species from alumina surface for each experiment by the different reagents was calculated using Equation 40.

After regenerating/or unloading the alumina bed, the regenerated alumina bed was reactivated by adjusting its pH to that of the virgin activated alumina by either using 0.1M

H_2SO_4 or 0.25M NaOH solution. For the continuous unloading experiments, the kinetic curves to describe the unloading of activated alumina bed were obtained by following the evolution of the aluminum silicate species at regular intervals. The trapezium rule was used to calculate the cumulative amount of species desorbed with time. The samples were filtered through a 0.2μm filter and analysed for silicon species, aluminum and calcium concentrations using ICP-AES.

4 RESULTS AND DISCUSSION

4.1 Investigation into alumina surface chemistry in solution

4.1.1 Dissolution and transformation behaviour of alumina in suspension

Figure 13 and Figure 14 show the results of the batch experiments carried out to determine the dissolution of activated alumina in deionised water and the gas condensate at room temperature and at a pH range of 8.3-9.0 as a function of time. The results show that the dissolution of activated alumina is higher for the finer particles compared to that of the activated alumina pellets for both the deionised water and the gas condensate. A maximum in Al concentration in solution was observed at the beginning of the fines dissolution compared to the alumina pellets dissolution. Although the experiments were conducted batch-wise, the Al concentration decreased after 30 minutes and 15 minutes for deionised water and gas condensate stream respectively. Furthermore, the aluminum dissolution was higher in gas condensate than in deionised water. A maximum Al concentration of about 1.2mg/l in deionised at a pH of 8.3 to 9.0 was observed compared to 7mg/l in gas condensate. The higher dissolution of Al in the gas condensate might be due to the formation of aluminate ($Al(OH)_4^-$) species from the hydrated activated alumina formed by some alumina particles in the alkaline region when in solution.

The maximum dissolution obtained initially for fines and nanoparticles experiments can be attributed to an increased particle surface area exposure to water as the particle size decreases. It has been shown that oxide (aluminum oxide) nanoparticles dissolution results in a maximum in Al concentration at the beginning which is followed by a decrease in Al concentration (Vogelsberger et al., (2008). The decrease in Al concentration observed can be assigned to the formation of a new phase as a result of dissolved Al precipitating out as suggested by Vogelsberger et al., (2007). However, the formation of a new phase was confirmed by Carrier et al., (2007). According to Carrier et al., (2007), the new phases observed was as a result of alumina dissolution in suspension followed by precipitation and alumina hydration through hydrolysis of Al-O bonds on the alumina surface.

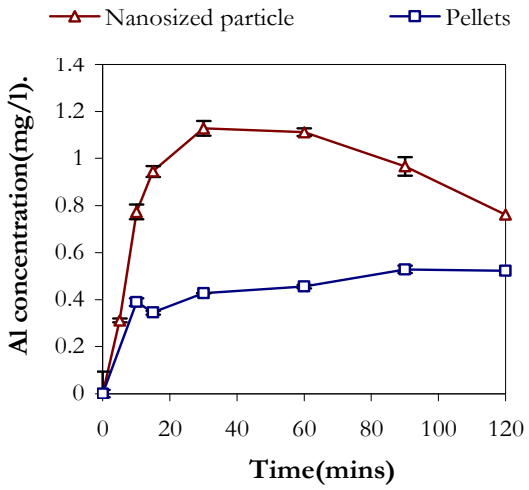

Figure 13: Dissolution kinetics of activated alumina in deionised water at room temperature and pH adjusted at 8.3 to 9.0.

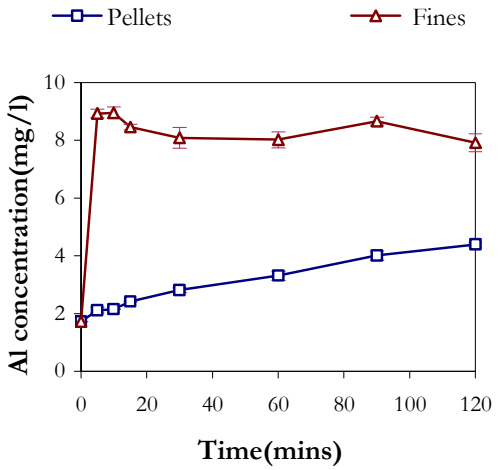

Figure 14: Dissolution kinetics of activated alumina in the gas condensate stream at room temperature and pH of 8.3 to 9.0 (2mg/l initial Al concentration).

Also, the change in particle size diameter as dissolution of the nanoparticles and fines progresses was investigated and is shown in Figure 15 and Figure 16. Figure 15 shows that for the first 30 minutes the particle diameter was decreasing. Figure 16 shows a decrease in particle diameter and number density in the first 20 minutes followed by an increase at 45 minutes calculated using Equation 4. The decrease in particle diameter and number density might be due to some alumina particles dissolution as suggested by the increase in Al concentration during the dissolution experiments for the first 30 minutes as shown in Figure 13. The increase in particle size after the first minutes of the experiments could be due to precipitation of aluminate species leached out from the hydrated alumina onto the solid particles of activated alumina as explained by the decrease in Al concentration after 30 minutes in Figure 13. The precipitated new phases might be amorphous aluminum hydroxide or bayerite which was found to be formed under alkaline conditions by Carrier et al., (2007). Since the point of zero charge of alumina lies in the pH range of 7 to 10 and this is the point of colloidal least stability (Goldberg et al., 1996; Yopps and Fuerstenau, 1964), the particle size increase is most likely due to the deposition of the colloids formed from the precipitating bayerite. However, the inconsistency in particle size diameter evolution noticed at 90 minutes and 60 minutes under the alkaline conditions could be due to hydrated/hydroxide phases re-dissolving back into solution.

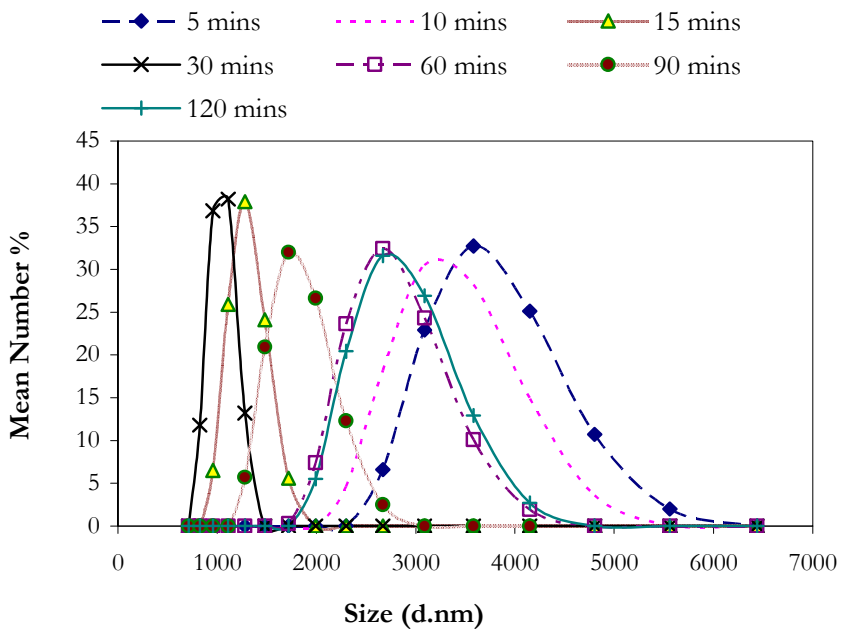

Figure 15: Change in particle size diameter during alumina fines dissolution in water.

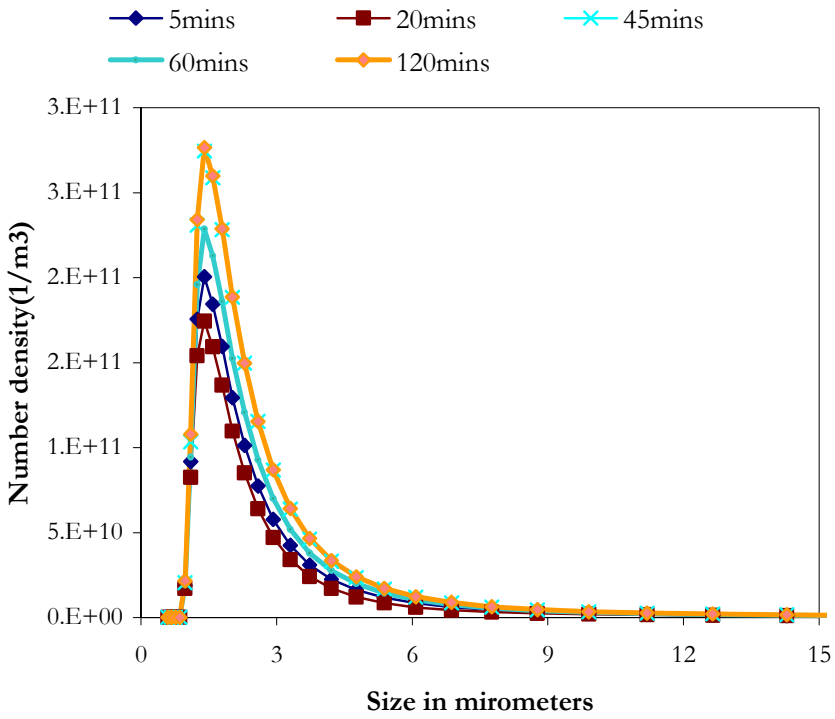

Figure 16: Particle size evolution during dissolution experiments

The activated alumina particles suspended in water at varying times from the dissolution experiments were dried at 60°C and analysed using XRD to investigate the formation of a new phase when alumina is in aqueous solution. Figure 17 shows the XRD patterns of activated alumina before (virgin alumina) and after suspension in deionised water at different times. The narrow diffraction peaks at about 21.9°, 23.7°, 32.4° and 47.6° emerged within 48 hours of immersing alumina in deionised water. The emerging new peaks were assigned to bayerite (PDF No. 00-020-0011, 01-074-1119, 01-077-0250 and 01-077-0114). The results are in agreement with studies by Carrier et al., (2007). Carrier and co-workers (2007) assigned the peaks to the formation of the hydroxide phases of aluminum through the hydrolysis of surface Al-O bonds and the dissolution followed by subsequent precipitation of the aluminum in the form of hydroxide.

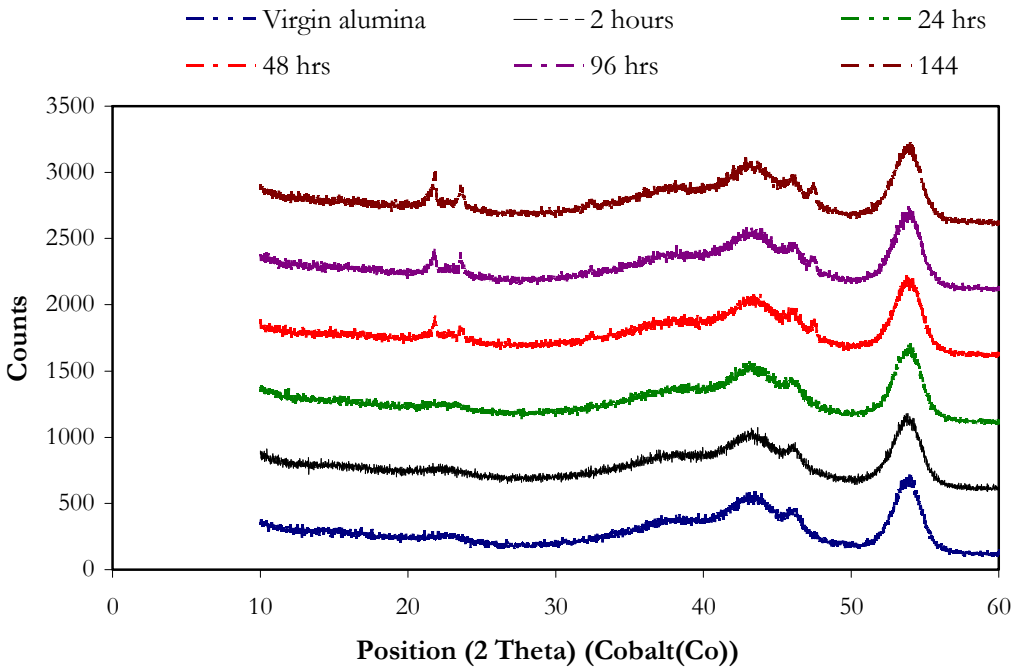

Figure 17: XRD patterns of alumina suspended in deionised water for different times.

4.1.2 Determination of activated alumina and silica zeta potential

Figure 18 and Figure 19 show the results of the batch experiments carried out to determine the point of zero charge of alumina and silica as a function of pH respectively. The results show the point of zero charge of activated alumina to be around a pH of 8.2. The activated alumina is positively charged below pH 8.2 and negatively charged for pH above 8.2 in both deionised water and 0.01M NaCl electrolyte. This substantiates the findings by other researchers who reported the point of zero charge of alumina to lie in the pH range of 7.0 - 10 (Goldberg et al., 1996; Yopps and Fuerstenau, 1964). The surface charge might be due to the differential loss of ions and the adsorption of charged particles (Kasprzyk-Horden, 2004; Stumm and Morgan, 1981) from solution since activated alumina undergoes transformation and dissolution when in solution as shown by Figure 13 and Figure 14. However, no point of zero charge was observed for silica though it is negatively charged for almost the entire pH range as shown in Figure 19.

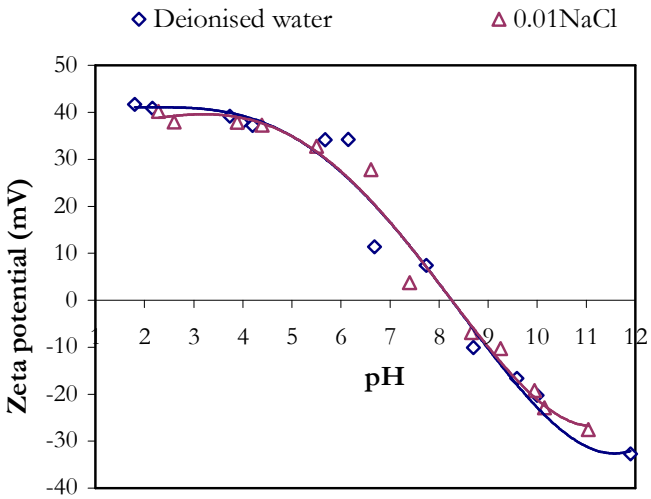

Figure 18: Zeta potential of alumina as a function of pH

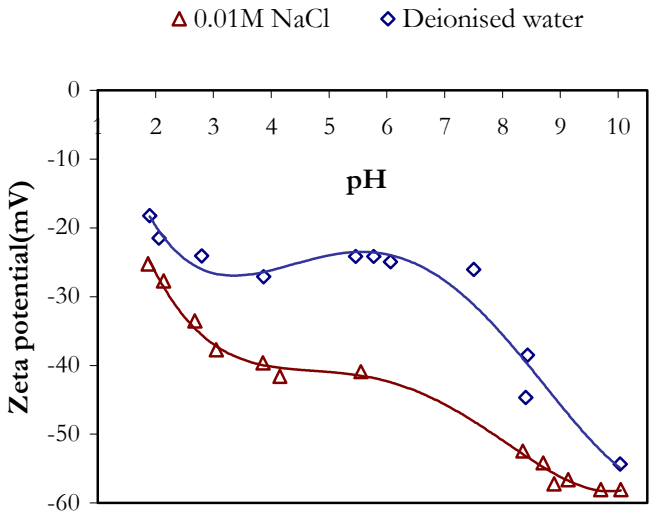

Figure 19: Zeta potential of silica as a function of pH

4.2 Understanding the mechanism(s) of aluminum silicate species removal by activated alumina

Alumina surface chemistry and species evolution in solution was used to propose the most likely removal mechanism(s) of Si and Ca from solution by alumina. Figure 13 to Figure 18 show the results obtained for the experiments carried out to investigate the alumina surface

chemistry in aqueous suspensions at a pH of 8.3 to 9.0. The results show that when the alumina was immersed in water, small amounts of alumina particles are hydrated and form aluminate ($Al(OH)_4^-$)species by dissolution (Figure 13) followed by precipitation of Al in the form of amorphous aluminum hydroxide or bayerite (Figure 17). This is also the case when the alumina is negatively charged above pH of 8.2 (Figure 18). Figure 19 shows that silica remains negatively charged for practically the entire pH range. Figure 9 and Figure 10 show the speciation of amorphous silica and amorphous aluminum hydroxide as a function of pH from the equilibrium equations extracted from Stumm and Morgan, 1996. Under alkaline conditions, silica exists as the reactive and colloidal form whilst aluminum exists as hydroxide complexes (ller, 1979). A schematic representation of the suggested removal mechanism(s) involved is summarised in Figure 20.

Batch experimental results on the uptake of Ca and Si by activated alumina from the synthetic solution and the gas condensate as a function of time are as shown in Figure 21 and Figure 22. Figure 23 shows the continuous experiment results to investigate the uptake of Si and Ca from the gas condensate by activated alumina in a packed bed column. Initially, a maximum removal of Si and Ca was observed which then levels off after treating 0.5 litres of gas condensate and remains relatively constant throughout the experiment. It was also observed that the aluminum concentration increases initially and then levels off throughout the experiment. The increase in Al concentration can be due to dissolution of Al due to small amounts of alumina particles which can start the reaction to form hydrated alumina and consequently aluminate species at higher pH values of greater than 8.0. The species removal trend suggests a change in the removal mechanism(s) during the course of the experiment. Activated alumina is used as an adsorbent in waste-water treatment (Kasprzyk-Hordern, 2004). The species removal trend suggests that the process of Si removal from the gas condensate cannot be attributed exclusively to an adsorption process, which if was the case, would show a gradual decline in Si and Ca removal with increasing volumes of gas condensate treated due to the saturation of the adsorption sites. Alumina when in solution reacts to form hydrated alumina followed by the leaching out of aluminate species into solution (Figure 13 and Figure 14). The aluminate species precipitate out as the hydroxide phases in suspension to form a hydroxylated alumina surface (Figure 17). This led to the suggestion that the maximum Si and Ca removal attained initially was as a result of a

combination of adsorption and precipitation (surface precipitation and bulk precipitation). The hydroxylated alumina surface could be acting as a seed and at the same time as an adsorbent, facilitating the uptake of both calcium and silica species. The continuous removal of Si and Ca throughout the experiment without the attainment of a break through point of zero percent removal suggests Si deposition on the already adsorbed Si to form a film (surface precipitation) though the adsorption sites were already taken up (Li and Stanforth, 2000, Iler, 1979).

Furthermore, Al ions in solution could be reacting with Si and Ca to form aluminosilicates in bulk solution (Matjie and Engelbrecht, 2007; Stumm, 1992). Al concentration from small amounts of alumina particles dissolution in gas condensate was as high as 7mg/l. Fresh gas condensate had concentrations of Si as high as 12mg/l. The two concentrations of Si and Al are already more than those which were found to cause solutions to be saturated with respect to aluminosilicates by Drever, 1988. Also, silicon species and aluminum are more stable in the polymeric form (ller, 1979). Thus, bulk precipitation of aluminosilicates is additionally a likely mechanism of Si and Ca removal together with surface precipitation and adsorption. Doucet et al., (2001) reported the formation of hydroxyaluminosilicates (HAS) though the mechanism of formation is not fully understood. As noted by Jardine and co-workers (1985) aluminosilicates such as kaolinite and montmorillonite preferentially adsorb either the polymeric or monomeric aluminum species. Hence, bulk precipitation (polymerisation) could be responsible for Al species equilibration in solution. As both alumina and silica are negatively charged at pH above 8.2, Ca removal could also be as a result of the electrostatic attraction.

Theoretically, Al addition into solution is expected to stop to indicate the complete coverage of the alumina surface. However, Al release into solution was continuous. This confirms alumina porosity and hydration with consequent formation of aluminate species under alkaline conditions being unconfined to the surface (Carrier et al., 2007; Hellmann, 1995).

On the other hand, Figure 21 shows that the concentrations of the scaling species in the synthetic stream were less than that of the gas condensate. Contrary to the gas condensate results, no alumina dissolution was observed in the experiments performed on synthetic solutions. However, on leaving the solution standing at room temperature for 8 days, the

deposition of a white precipitate was observed. This could be due to a slow polymerisation of the monomeric silica and aluminum into amorphous silica and amorphous aluminum hydroxide (Krauskopf, 1956).

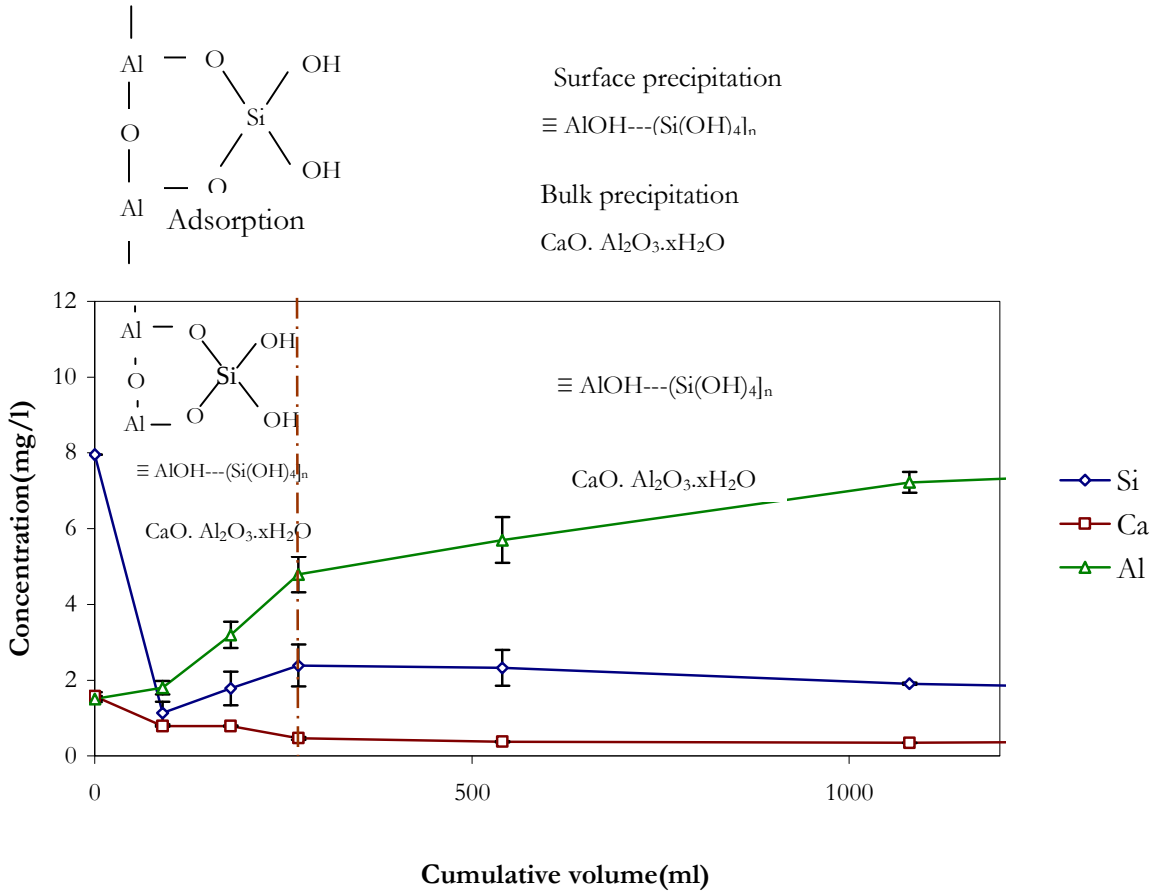

Figure 20: Schematic summary of the most likely Si, Ca removal mechanism(s) by activated alumina with cumulative gas condensate volume

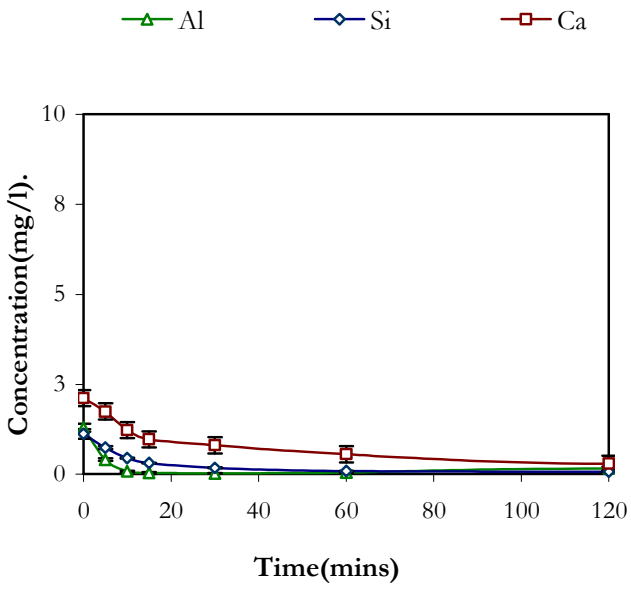

Figure 21: Concentrations of Si, Ca and Al in the synthetic solution contacted with activated alumina in a batch-wise mode as a function of time.

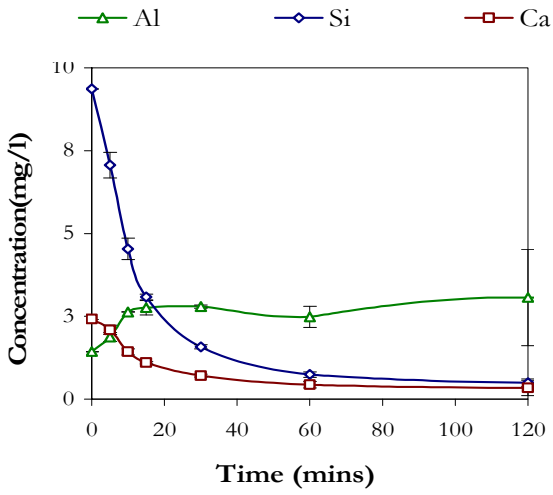

Figure 22: Concentrations of Si, Ca and Al in gas condensate contacted with activated alumina in a batch-wise operation mode as a function of time.

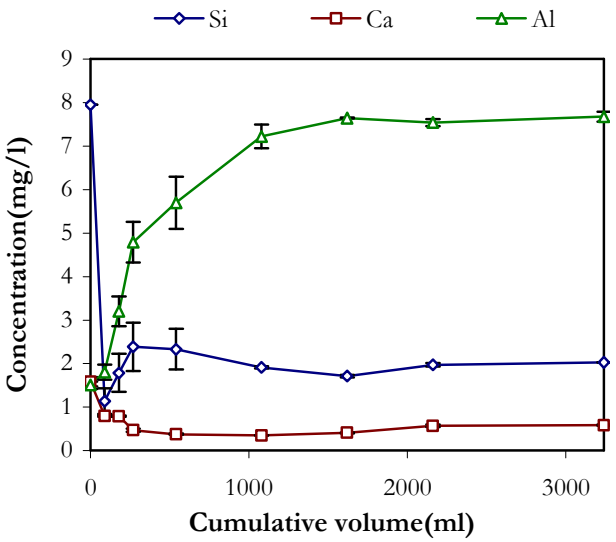

Figure 23: Concentrations of Si, Ca and Al in a continuously fed gas condensate through a packed bed of activated alumina (T=40°C, 6 minutes residence time)

The loaded alumina was also analysed using Scanning Electron Microscope (SEM) and Energy Dispersive Spectroscopy (EDS) as shown in Figure 24 and Figure 25. Analysis of the results shown in Figure 24 did not detect the presence of either of the aluminosilicate species (calcium and silica). This might be due to the fact that the species concentrations are below the detection limits of the analytical instrument. The SEM pictures show less agglomerates of tiny particles in A and B compared to C. The larger agglomerates in picture C could be precipitates of the aluminosilicates deposited on alumina surface. The slightly bigger and smooth agglomerates in de-ionised water (picture B) could be an indication of the formation of a crystalline hydroxide phase. However, the analysis of a solid obtained during the unloading of loaded alumina showed the presence of silica as shown in Figure 39.

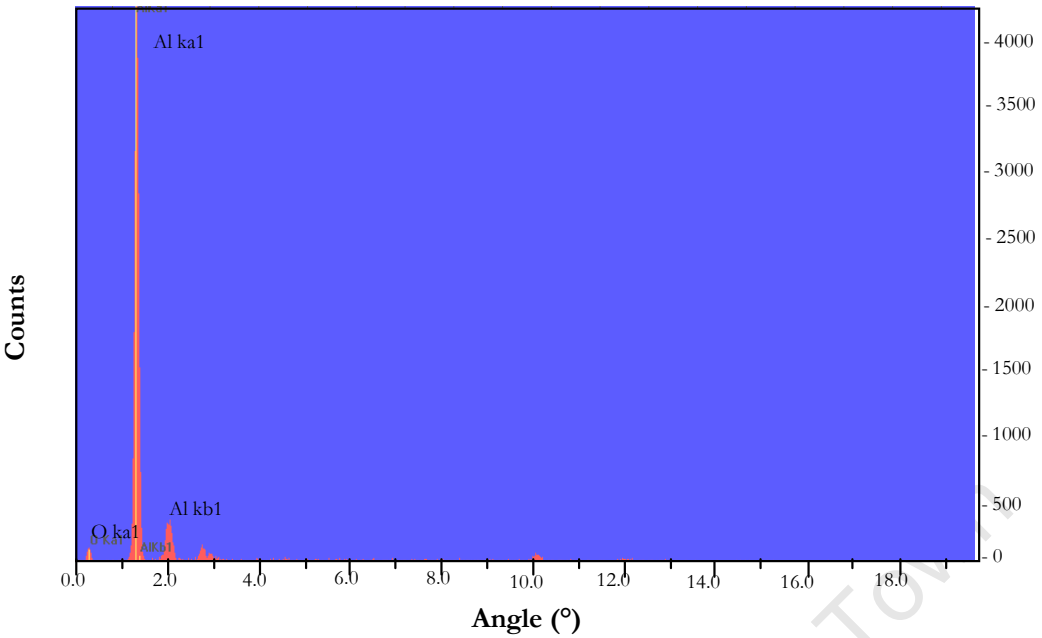

Figure 24: Energy dispersive spectroscopy analysis of activated alumina pellets saturated with aluminum silicate species

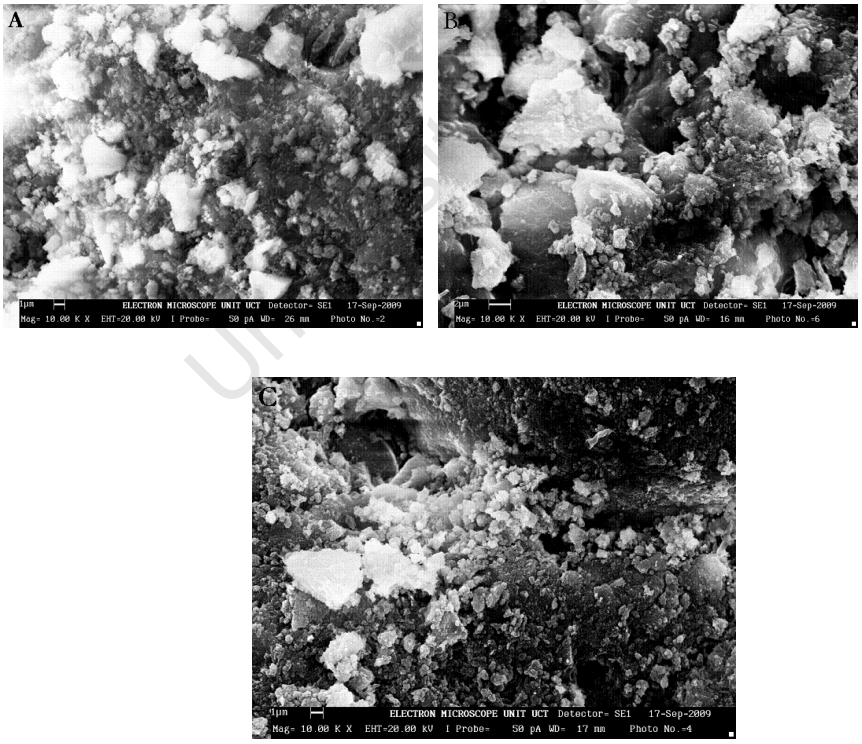

Figure 25: Scanning Electron Microscopy photographs for activated alumina. **A**- Virgin alumina; **B**- alumina suspended in de-ionised water: **C**- alumina suspended in gas condensate

4.3 Investigation into the unloading of the loaded bed of activated alumina by aluminum silicate species (regeneration)

4.3.1 Determination of the alumina-reagent ratio to be used

Firstly, gas condensate was continuously run through a packed bed of virgin activated alumina in order to load it with the aluminum silicate species in a jacketed column at 1ºC±40ºC. The loaded activated alumina was then washed using varying volumes of 0.1M H_2SO_4. Figure 26 shows the percentage removal of the Si and Ca species on the primary axis as well as the Al species removal on the secondary y-axis for an unused alumina sample when treating a cumulative gas condensate volume of 8 litres at an alumina dosage of 25g/l and a residence time of 6 minutes.

The results show that the Si removal levels off at ~70% after treating 2 litres of gas condensate and remains relatively constant until a volume of 8 litres were treated. This suggests that the process of the Si removal from the gas condensate cannot be attributed exclusively to an adsorption process which if was the case, would show a decline in the percentage Si removal with increasing volumes of gas condensate treated due to the saturation of the adsorption sites. This trend in Si removal could be due to the continuous removal of dissolved silica by a surface reaction with the OH groups of the hydrated phases of the alumina, as well as the OH groups of the Si on the alumina surface as suggested by Hanzlicek, Steinerova-Vondrakova (2002). Therefore, this shows that surface precipitation plays a significant role in the removal of the aluminum silicate species (Iler, 1979). Hence, the regeneration of the activated alumina adsorption sites may not be as critical as initially envisaged. Conversely, the aluminum showed a negative removal implying that aluminum was being leached into solution. This negative removal of aluminum is a result of small particles of alumina dissolution as found in the alumina chemistry experiments. Furthermore, a correlation in the removal trend of Ca and Si was observed suggesting a link between Si and Ca in solution.

After treating a cumulative gas condensate volume of 8 litres, batch-wise regeneration of alumina was carried out using different volumes of 0.1M sulphuric acid to investigate the alumina to reagent ratio to be used. As shown in Figure 28 the percentage of Si desorbed from the used alumina after 120 minutes is approximately 30%, 50% and 58% using 1, 2 and

3 litres of 0.1M sulphuric acid respectively. In comparison to the 30% Si desorption attained for 1l acid, this meant a 20% and 28% increase in Si desorption for 2l and 3l of 0.1M sulphuric acid used respectively. From the results the reaction time required for desorption equilibrium was about 60 minutes when 1l and 2l acid was used. However, for 3l, desorption equilibrium was not attained even after 120 minutes of the experiment. The failure to attain equilibrium could be as a result of the slow Si release into solution caused by the reduced silica concentration on the alumina surface as dissolution proceeds. The increase in the amount of Si desorbed with an increase in volume of 0.1M sulphuric could be due to Si reaching its solubility equilibrium since a larger volume of liquor means more Si desorption to reach the solubility equilibrium. As shown by Figure 27, at around 60 minutes reaction time the concentration of Si was about 9.1mg/l. This was in agreement with the review by Iler, (1979) on the reduction of silica solubility to below 9.5ppm in the presence of trace amounts of alumina or iron at 20°C. Hence, an alumina to cleaning reagent ratio of not more than 1g alumina/40ml reagent was used during the regeneration experiments.

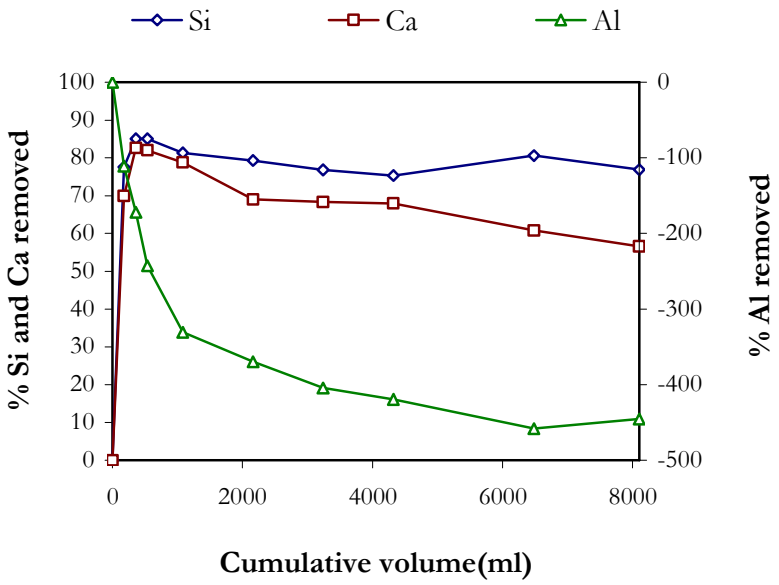

Figure 26: Percentage of Si, Ca, and Al removed from the gas condensate by virgin activated alumina (25g/L alumina dosage, 6 mins residence time)

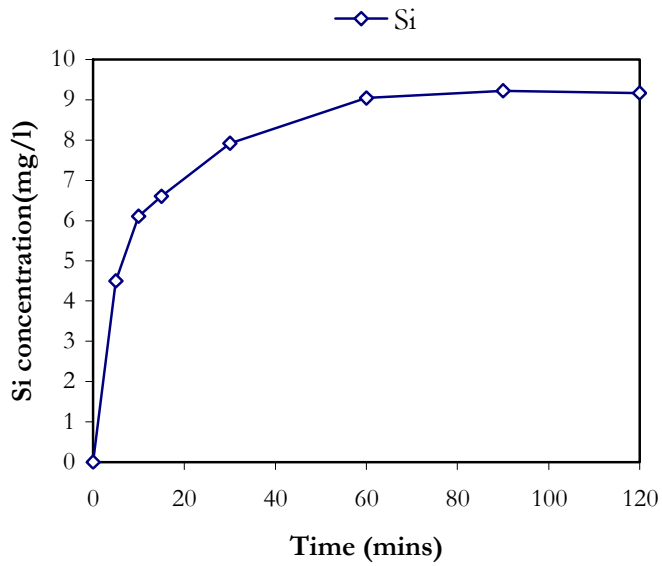

Figure 27: Concentrations of Si in washing solution attained during batch-wise unloading of saturated activated alumina using 1 litre of 0.1M H_2SO_4 as a function of time (50g alumina)

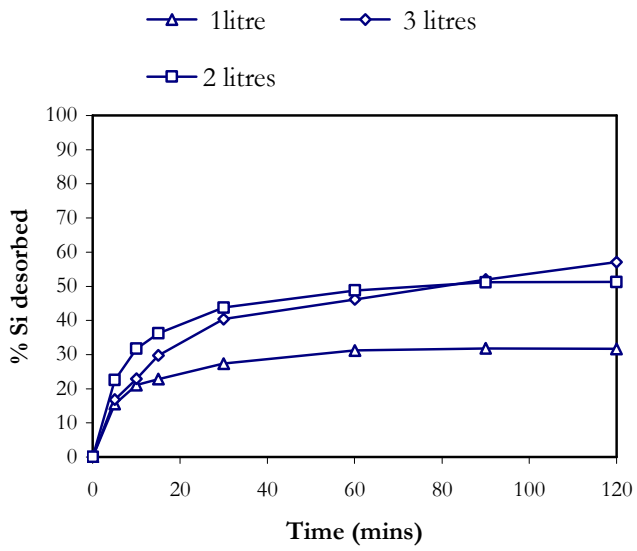

Figure 28: Percentage of Si desorbed from a saturated bed of activated alumina during regeneration using different volumes of washing solution (0.1M H_2SO_4) as a function of time (50g alumina).

4.3.2 Investigations into the use of the various cleaning reagents to regenerate alumina

Table 2 gives the various concentrations for the different reagents used to regenerate alumina. The reagent solutions used were sodium hydroxide solution (NaOH), sulphuric acid solution (H_2SO_4) and sodium gluconate solution ($C_6H_{11}NaO_7$) of varying concentrations as shown in Table 2. The % Si unloading and the % aluminum dissolution after a reaction time of 120 minutes using the different washing reagents of varying concentrations are shown in Figure 31 and Figure 32 respectively. For the three reagents, it was observed that both % Si unloading and % Al dissolution increases with an increase in reagent concentration. Considering the highest reagents concentrations used, 0.65M of NaOH and 0.1M H_2SO_4 showed a percent Si unloading of approximately 50% whereas 0.25M sodium gluconate gave approximately 5% Si unloading. However, for these high concentrations of reagents used during the experiments, NaOH showed the highest Al dissolution of about 2.5 % compared to that of H_2SO_4 and sodium gluconate which were about 0.5% and 0.3% respectively. This suggests that more particles of alumina are hydrated and hence more aluminate species leached into solution under alkaline conditions or rather 0.65M NaOH is highly concentrated for regenerating alumina. The higher Al dissolution at high pH values could have been promoted by the high concentration of OH groups which were binding on the surface complex and the co-existence of deprotonated hydroxylated silica and alumina groups (Stumm, 1997; Hellmann, 1995). The point of zero charge of alumina was found to be around the pH of 8.2 whereas silica was negatively charged for almost the entire pH range during alumina zeta potentials measurements. Hence, the observed small amounts of alumina particles dissolution in both alkaline and acidic conditions is in agreement with the earlier studies that found that, the dissolution rates of oxides and silicates below their pH of point of zero charge increase with decreasing pH and increases with increasing pH in the alkaline region (Stumm, 1997).

Sodium gluconate is a weak acid; hence the lower unloading of silica due to very low H^+ concentrations to hydrolyze the silanol bonds. The dissolution of small amounts of alumina particles was not desired in this study and hence, the 0.65M NaOH was not suitable to

regenerate the alumina. As the used concentrations of sodium gluconate did not desorb much of silicon species, it was not used for the continuous regeneration experiments.

Table 2: Various concentrations of the different reagents used to regenerate saturated activated alumina

Reagent	Concentration used
NaOH(aq)	0.025M, 0.25M and 0.65M
H_2SO_4(aq)	0.01M, 0.025M and0.1M
$C_6H_{11}NaO_7$(aq)	0.005M, 0.05M and 0.25M

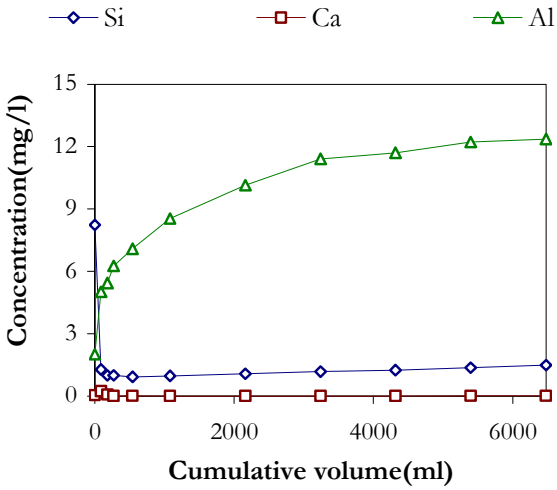

Figure 29: Concentrations of Si, Ca and Al in a continuously fed gas condensate through a packed bed of activated alumina (25g/l alumina dosage, 6 minutes residence time).

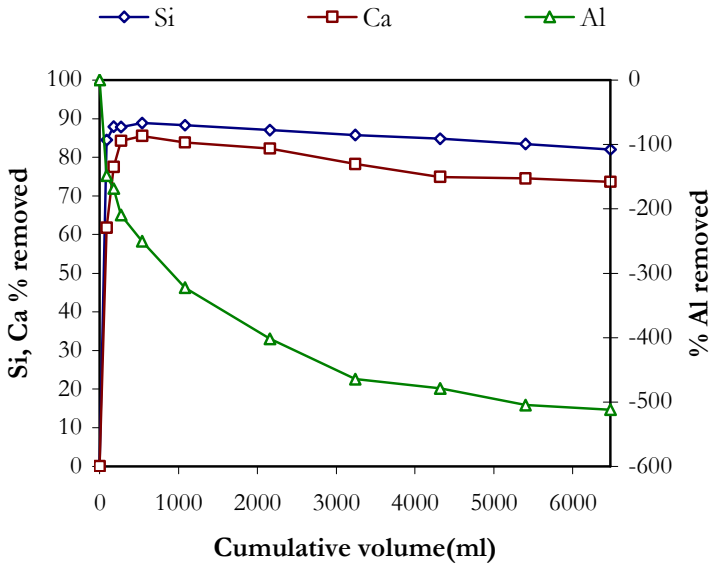

Figure 30: Percentage of Si, Ca, and Al removed from the gas condensate by virgin activated alumina (25g/L alumina dosage, 6 mins residence time).

.

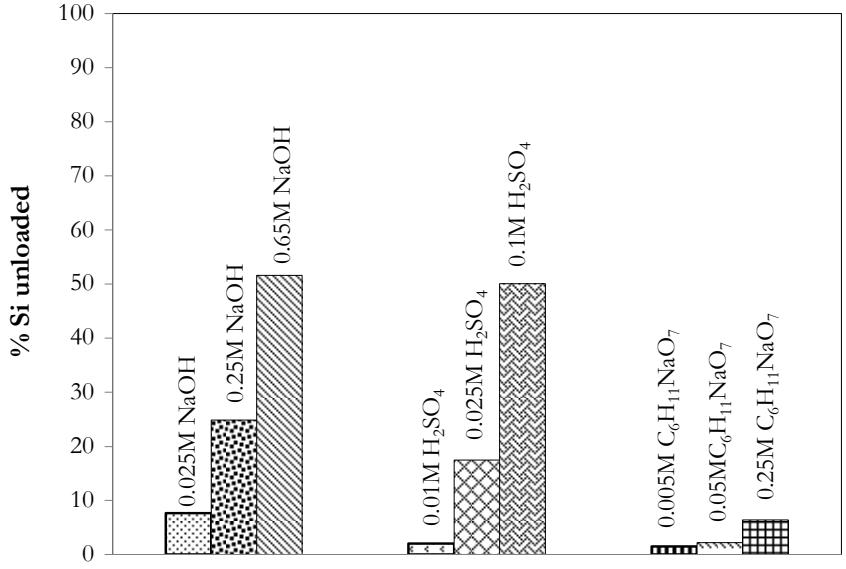

Figure 31: Percentage of Si unloaded from loaded alumina at the end of the experiments for the various cleaning reagents for the different concentrations used (120 minutes reaction time).

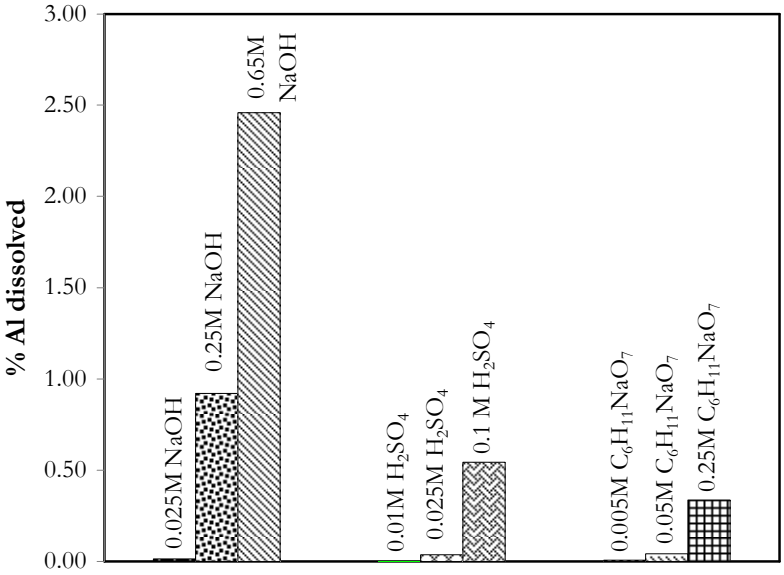

Figure 32: Percentage of Al dissolved from the loaded alumina in the different cleaning reagents of varying concentrations at the end of the experiments (120 minutes reaction time)

4.3.3 Regeneration of alumina in a continuous mode operation

For the continuous regeneration experiments, the activated alumina was firstly loaded with the aluminum silicate species at an activated alumina dosage of 25g/l and 6 minutes residence time as shown in Figure 33 and Figure 34. The loaded alumina was then continuously regenerated using 0.1M H_2SO_4 and 0.25M NaOH solutions at a residence time of 3 minutes. These experiments were carried out to investigate whether the silica solubility equilibrium was the limiting factor for silica desorption. The evolution of the aluminum silicate species as a function of time for the two reagents used is as shown in Figure 35 and Figure 36. Figure 37 compares the effect of the 0.1M H_2SO_4(aq) and the 0.25M NaOH (aq) on desorbing silicon species. The results show that most of the desorbable aluminosilicate species were desorbed within the first 15 minutes. Furthermore a higher silica unloading was achieved for the 0.1M H_2SO_4(aq) compared to the 0.25M NaOH (aq). This higher desorption within the first 15 minutes was due to the higher concentrations of the adsorbate on the surface at the beginning of the experiments (Stumm, 1997). The decline in Si desorption after 15 minutes was due to the decrease in silica concentration on the alumina

surface. However, lower Si unloading for 0.25M NaOH might be attributed to the fact that the solution was not highly alkaline to provide enough OH groups to promote dissolution since the binding of OH on the surface complex is the one which facilitates dissolution. Also, the lower rate of Si desorption reported in the alkaline medium compared to that with H_2SO_4 could be as a result of the Si-O-Si bond hydrolysis being followed by its dehydroxylation as suggested by Pelmenschikov et al. (2001).

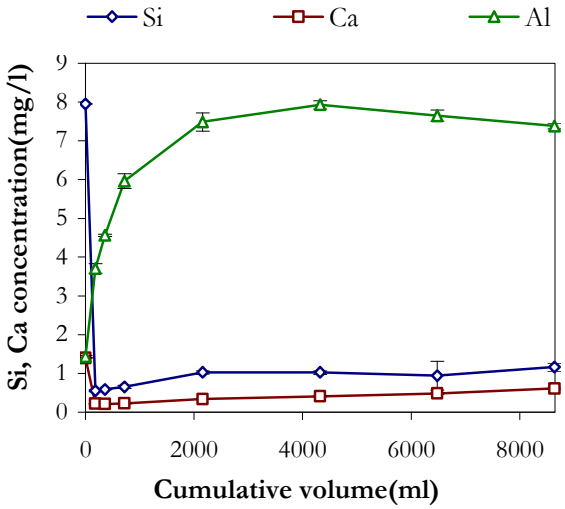

Figure 33: Concentrations of Si, Ca and Al in a continuously fed gas condensate through a packed bed of activated alumina (25g/L alumina dosage, 6 minutes residence time)

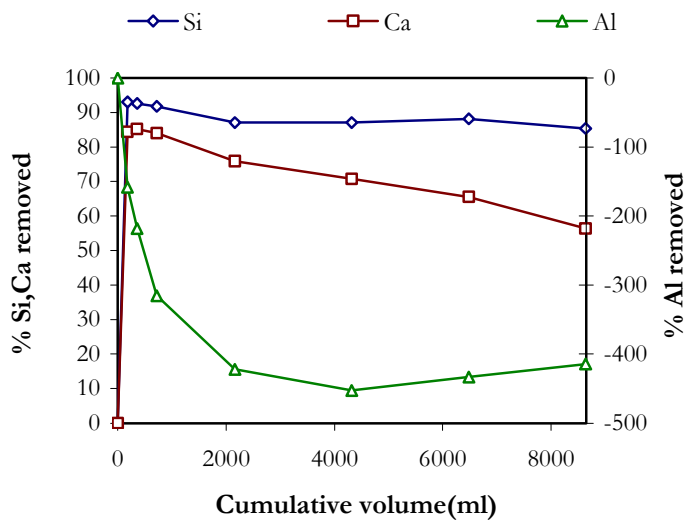

Figure 34: Percentage of Si, Ca, and Al removed from the gas condensate by virgin activated alumina (25g/L alumina dosage, 6 mins residence time).

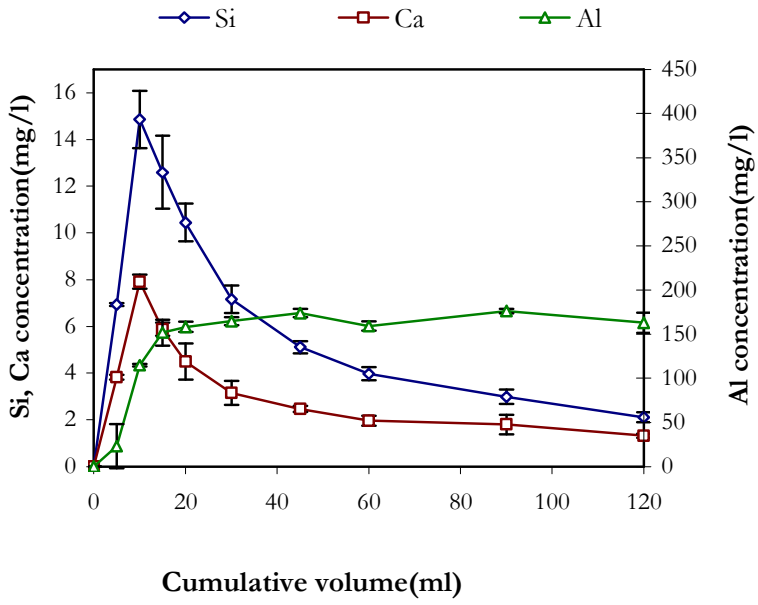

Figure 35: Concentrations of Si, Ca and Al in washing solution attained when using 0.1M H_2SO_4 to regenerate the loaded activated alumina as a function of time (3 minutes residence time)

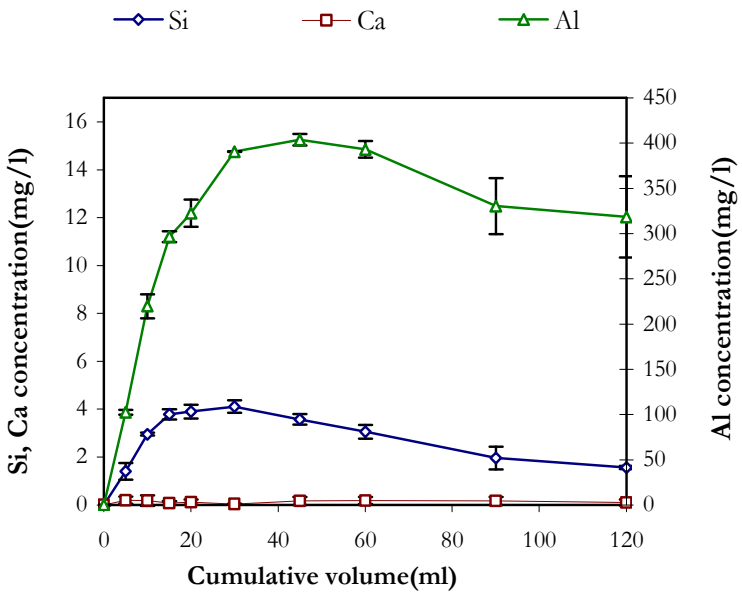

Figure 36: Concentrations of Si, Ca and Al in washing solution attained when using 0.25M NaOH to regenerate the loaded activated alumina as a function of time (3 minutes residence time)

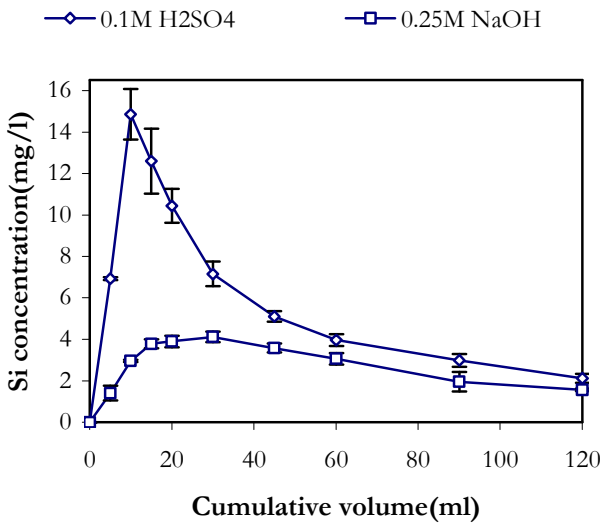

Figure 37: Concentrations of Si removed from loaded alumina in washing solution attained when using 0.1M H_2SO_4 and 0.25M NaOH to regenerate the loaded activated alumina as a function of time (3 minutes residence time)

Figure 38 shows that the overall % Si removed from loaded alumina when using 0.1M H_2SO_4 and 0.25M NaOH was approximately 70% and 40% respectively. During batch regeneration the overall Si desorption of 50% and 24% were obtained for 0.1M H_2SO_4 and 0.25M NaOH respectively. The dissolution curves (Figure 28 and Figure 37) suggest that Si desorption is surface controlled (Stumm and Morgan, 1996).

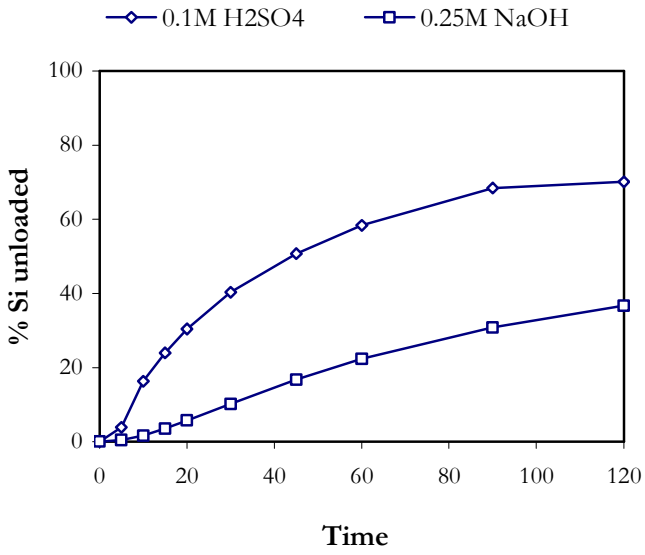

Figure 38: Cumulative percentage Si unloaded from loaded alumina when regenerating loaded alumina using 0.1M H_2SO_4 and 0.25M NaOH (3 minutes residence time, and 50g loaded alumina).

During the washing experiments, fines were also formed and these were analysed using the SEM and the EDS in order to find their composition and morphology. The results are shown in Figure 39 and Table 3. Si was detected as one of the constituent elements, contrary to the mechanism(s) experiments.

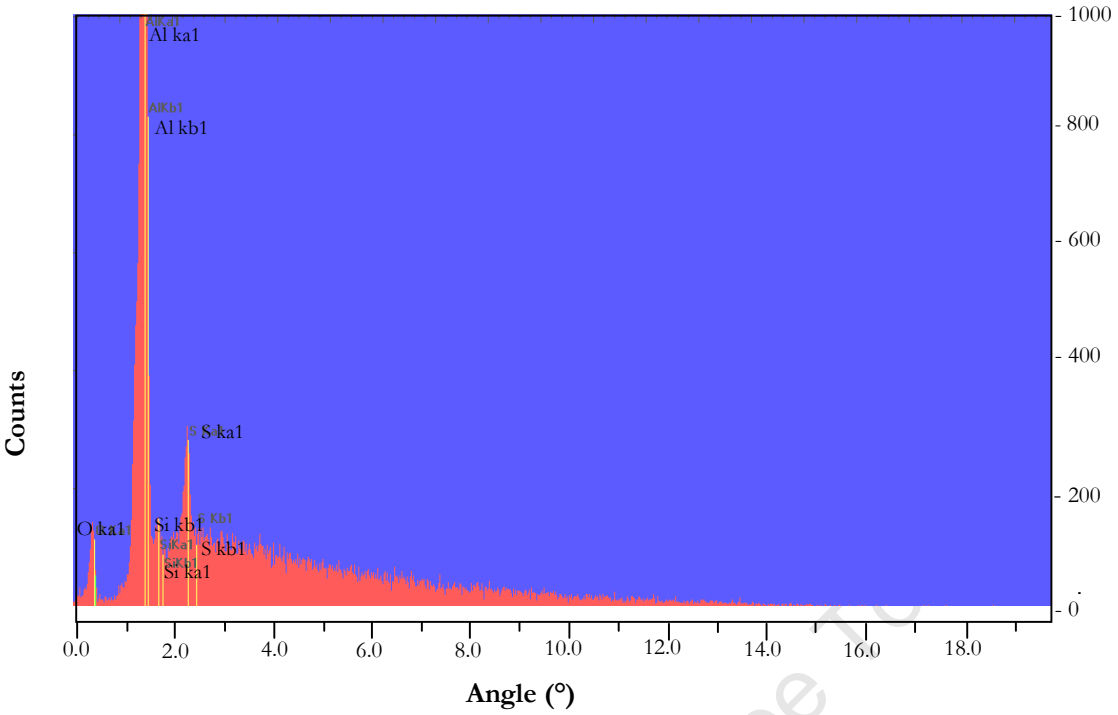

Figure 39: Energy Dispersive Spectroscopy (EDS) analysis of fines formed during washing loaded alumina by 0.1M H_2SO_4

Table 3: The Energy Dispersive Spectroscopy (EDS) percentage element analysis of fines formed during washing of loaded alumina

Element	Weight %	Atomic %
O	22.70	33.41
Al	68.96	60.18
Si	2.84	2.38
S	5.49	4.03

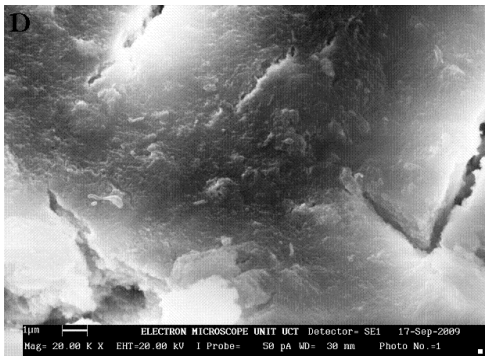

Figure 40: Scanning Electron Microscope photograph of the fines produced during washing of loaded alumina using 0.1M H_2SO_4

4.3.4 Alumina loading capacity recovery

Figure 41 to Figure 44 show the results for the second loading of washed alumina carried out to determine the recovery of alumina loading capacity as a result of both acid and caustic regeneration. The second loading of the washed alumina by 0.1M H_2SO_4 and 0.25M NaOH gave a maximum Si removal of 86% and 75% respectively (Figure 42 and Figure 44). It was also observed that the removal was also followed by a levelling off in the Si removal as a function of the cumulative gas condensate volume treated as in the loading of virgin alumina. The first loading of virgin alumina levelled off at about 84% and hence it can be concluded that washing the loaded alumina by either acid or base does not reclaim the loading capacity of alumina. The amount of the Si and Ca removed continued from were it ended after the first loading. This could be attributed to the removal of the scaling species being predominantly a surface precipitation process after the initial adsorption process. This is evident in the continued removal of Si and Ca without reaching a breakthrough point during the second loading too. As such, the washing serves only to remove the successive layers of the aluminosilicate films which were precipitated on alumina surface and not to recover the adsorption sites on the alumina surface. Hence, there is no significant benefit of regenerating the alumina in terms of improving the performance of the removal of scaling species by the regenerated alumina. The unloading of the scaling species off the alumina surface would however benefit the process in terms of reducing the increase in pressure drop in the bed that could result from a reduction in the interstitial spaces between the

alumina pellets with the cumulative increase in the amount of silicates precipitating on the surface over time.

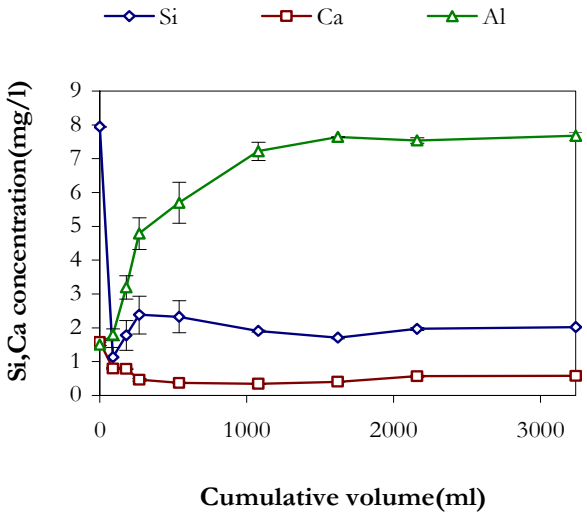

Figure 41: Concentrations of Si, Ca and Al in a continuously fed gas condensate through a packed bed of activated alumina previously washed using 0.1M H_2SO_4 (6 minutes residence time)

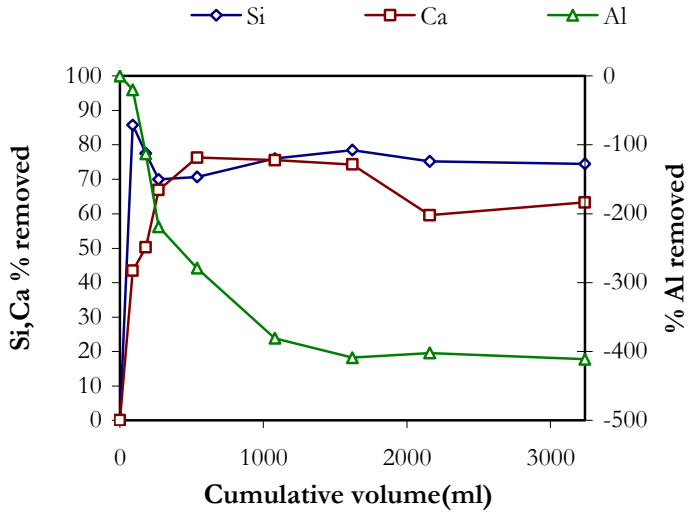

Figure 42: Percentage of Si, Ca and Al removed from gas condensate by loaded alumina which was previously washed using 0.1M H_2SO_4 (6 minutes residence time)

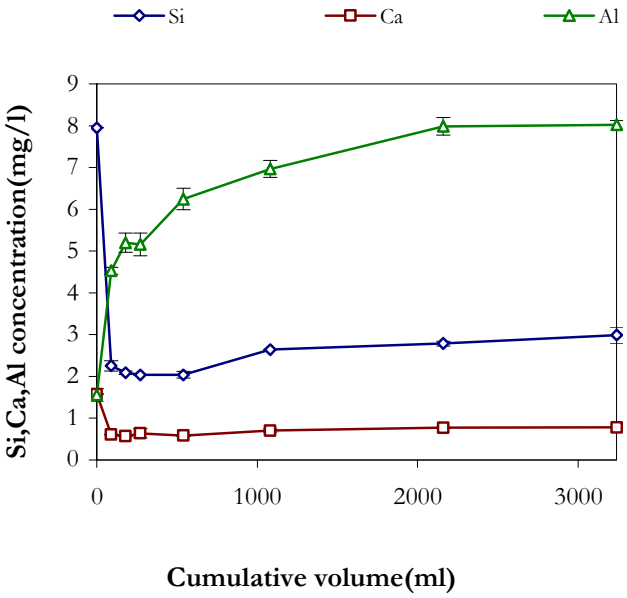

Figure 43: Concentrations of Si, Ca and Al in a continuously fed gas condensate through a packed bed of activated alumina previously washed using 0.25M NaOH (6 minutes residence time)

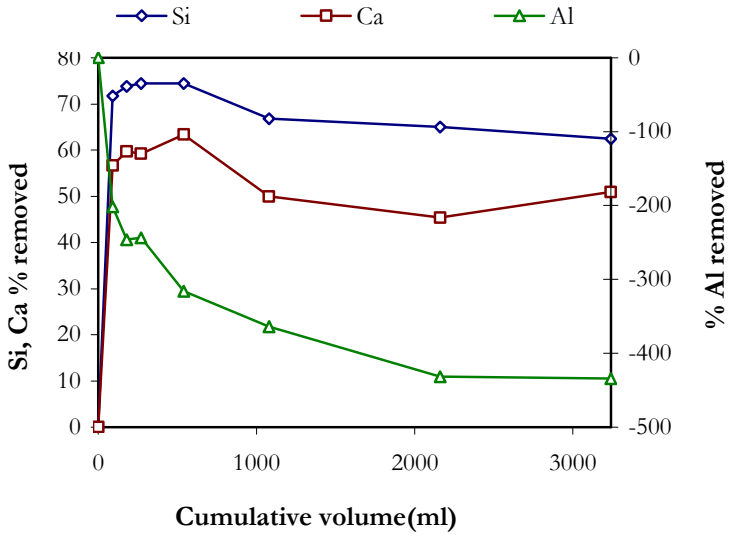

Figure 44: Percentage of Si, Ca and Al removed from gas condensate by loaded alumina which was previously washed using 0.25M NaOH (6 minutes residence time)

5 CONCLUSIONS

i. Small amounts of alumina particles react to form the hydrated alumina and subsequently the dissolution/or leaching out of the aluminate species into solution. However, the degree of dissolution is a function of particle size. The aluminate species consequently precipitate out as the hydroxide phases as a result of the solution being supersaturated.

ii. Activated alumina is porous and its hydration is not limited to the surface hence the continued release of Al into solution throughout the experiments.

iii. The pH of point of zero charge for alumina is 8.2, implying that under a pH range of 8.3 - 9.0, alumina is negatively charged. Also, silica is negatively charged for pH greater than 2. As a result the reactions between silica and alumina are not due to electrostatic attraction. The most likely interaction is as a result of surface complexation.

iv. It can also be concluded that the removal of silicon species from the gas condensate stream and natural waters is most likely due to a combination of adsorption and precipitation (bulk and surface enhanced precipitation). Surface precipitation being the predominant mechanism of silica removal in the systems.

v. The degree of regeneration can be measured by the extent to which the adsorbed species are desorbed from the adsorbent surface. Both sulphuric acid and sodium hydroxide solutions can be used to unload silica from the loaded alumina. However, the extent of desorption is a function of the acid and base concentration and adsorbate concentration.

vi. However, the benefit of regenerating the activated alumina is quantified by the improvement in the removal of the scaling species from gas condensate using the regenerated alumina during the second loading. From the results, there is no significant benefit of regenerating the alumina in terms of improving the performance of the aluminosilicate species removal by the regenerated alumina. The unloading of the scaling species off the alumina surface would however benefit the process in terms of reducing the increase in pressure drop in the bed that would result from a reduction in the interstitial spaces between the alumina pellets with the cumulative increase in the amount of silicates precipitated on the alumina surface over time.

vii. The unloading of the aluminum silicate species from the surface by either acid or base is highly dependent on the surface concentration of the silicates. Hence, the dissolution is surface controlled.

6 RECOMMENDATIONS

i. Experimental studies must be conducted to investigate the extent of scaling as a result of the aluminum dissolved into solution during alumina regeneration in the downstream processes.

ii. In order to reduce the likelihood of scaling by the aluminum silicate species remaining in the stream after running the stream through alumina, the downstream processes must be carried out at pH higher than 9.0.

iii. More experiments need to be conducted at varying volumetric flow rates in order to establish the effect of residence time on silicates unloading/dissolution in the packed bed column.

7 REFERENCES

Berkowitz, J., Anderson, M.A. & Graham, R.C. 2005, "Laboratory investigation of aluminum solubility and solid-phase properties following alum treatment of lake waters", *Water Research,* vol. 39, no. 16, pp. 3918-3928.

Birchall, J.D. 1994, *Silicon-Aluminum interactions in biology.*, American Chemical Society.

Bouguerra, W., Ben Sik Ali, M., Hamrouni, B. & Dhahbi, M. 2007, "Equilibrium and kinetic studies of adsorption of silica onto activated alumina", *Desalination,* vol. 206, no. 1-3, pp. 141-146.

Bouguerra, W., Mnif, A., Hamrouni, B. & Dhahbi, M. 2008, "Boron removal by adsorption onto activated alumina and by reverse osmosis", *Desalination,* vol. 223, no. 1-3, pp. 31-37.

Bremere, I., Kennedy, M., Mhyio, S., Jaljuli, A., Witkamp, G. & Schippers, J. 2000, "Prevention of silica scale in membrane systems: removal of monomer and polymer silica", *Desalination,* vol. 132, no. 1-3, pp. 89-100.

Cama, J., Metz, V. & Ganor, J. 2002, "The effect of pH and temperature on kaolinite dissolution rate under acidic conditions", *Geochimica et Cosmochimica Acta,* vol. 66, no. 22, pp. 3913-3926.

Carrier, X., Marceau, E., Lambert, J. & Che, M. 2007, "Transformations of γ-alumina in aqueous suspensions: 1. Alumina chemical weathering studied as a function of pH", *Journal of Colloid and Interface Science,* vol. 308, no. 2, pp. 429-437.

Chen, C.A. & Marshall, W.L. 1982, "Amorphous silica solubilities IV. Behavior in pure water and aqueous sodium chloride, sodium sulfate, magnesium chloride, and magnesium sulfate solutions up to 350°C", *Geochimica et Cosmochimica Acta,* vol. 46, no. 2, pp. 279-287.

Chida, T., Niibori, Y., Tochiyama, O., Mimura, H. & Tanaka, K. 2007, "Deposition rates of polysilicic acid with up to 10^{-3} M calcium ions", *Applied Geochemistry,* vol. 22, no. 12, pp. 2810-2816.

Doucet, F.J., Schneider, C., Bones, S.J., Kretchmer, A., Moss, I., Tekely, P. & Exley, C. 2001, "The formation of hydroxyaluminosilicates of geochemical and biological significance", *Geochimica et Cosmochimica Acta,* vol. 65, no. 15, pp. 2461-2467.

Drever, J.I. 1988, "The geochemistry of natural waters." in , 2nd edn, Prentice Hall, Englewood, N. J, .

Exley, C. & Birchall, J.D. 1992, "Hydroxyaluminosilicate formation in solutions of low total aluminum concentration", *Polyhedron,* vol. 11, no. 15, pp. 1901-1907.

Fournier, R.O. & Rowe, J.J. 1977, "The solubility of amorphous silica in water at high temperatures and high pressures", *American Mineralogist,* vol. 62, pp. 1052-1056.

Frank, R.S. 2003, *Handbook of water and wastewater treatment plant operations.* CRC Press.

Gabelich, C.J., Chen, W.R., Yun, T.I. & Coffey, B.M. 2005, "The role of dissolved aluminum in silica chemistry for membrane processes", *Desalination,* vol. 180, pp. 307-319.

Gallup, D.L., Sugiaman, F., Capuno, V. & Manceau, A. 2003, "Laboratory investigation of silica removal from geothermal brines to control silica scaling and produce usable silicates", *Applied Geochemistry,* vol. 18, pp. 1597-1672.

Ghorai, S. & Pant, K.K. 2005, "Equilibrium, kinetics and breakthrough studies for adsorption of fluoride on activated alumina", *Separation and Purification Technology,* vol. 42, no. 3, pp. 265-271.

Goldberg, S. 2002, "Competitive adsorption of arsenate and arsenite on oxides and clay minerals.", *Soil Science Society of America,* vol. 66, pp. 413-421.

Goldberg, S., Davis, J.A. & Hem, J.D. 1996, "The surface chemistry of aluminum oxides and hydroxides" in *The Environmental Chemistry of Aluminum*, ed. G. Sposito, Second Edition, Lewis Publishers, Boca Raton, pp. 271-318.

Hanzlicek, T. & Steinerova-Vondrakova, M. 2002, "Investigation of dissolution of aluminosilicates in aqueous alkaline solution under laboratory conditions.", *Ceramics,* vol. 46, no. 3, pp. 97-103.

Hellmann, R. 1995, "The albite-water system: Part II. The time-evolution of the stoichiometry of dissolution as a function of pH at 100, 200 and 300°C", *Geochimica et Cosmochimica Acta,* vol. 59, pp. 1669-1697.

Hohl, H. & Stumm, W. 1976, "Interaction of Pb^{2+} with hydrous γ-Al_2O_3", *Journal of Colloid and Interface Science,* vol. 55, no. 2, pp. 281-288.

Houston, J.R., Herberg, J.L., Maxwell, R.S. & Carroll, S.A. 2008, "Association of dissolved aluminum with silica: Connecting molecular structure to surface reactivity using NMR", *Geochimica et Cosmochimica Acta,* vol. 72, no. 14, pp. 3326-3337.

Huang, C. & Stumm, W. 1973, "Specific adsorption of cations on hydrous γ-Al2O3", *Journal of Colloid and Interface Science,* vol. 43, no. 2, pp. 409-420.

Iler, R.K. 1979, *The chemistry of silica: solubility, polymerisation, colloid and surface properties and biochemistry,* Willey-Interscience, New York.

Ingram-Jones, V.J., Slade, S.C.T., Davis, T.W., Southern, J.C. & Salvador, S. 1996, "Dehydroxylation sequences of gibbsite and boehmite: study of differences between

soak and flash calcination and of particle-size effects", *Journal of Material Chemistry,* vol. 6, pp. 73-79.

Janusz, W., Patkowski, J. & Chibowski, S. 2003, "Competitive adsorption of Ca (ll) and Zn (ll) ions at monodispersed SiO_2/electrolyte solution interface", *Journal of Colloid and Interface Science,* vol. 266, pp. 259-268.

Jardine, P. M., Zelazny, L. W., Parker, J. C. 1985, *Mechanisms of Aluminum Adsorption on Clay Minerals and Peat*[1], Soil Science Society of America, USA.

Kasprzyk-Hordern, B. 2004, "Chemistry of alumina, reactions in aqueous solution and its application in water treatment", *Advances in Colloid and Interface Science,* vol. 110, no. 1-2, pp. 19-48.

Kirk Othmer, *Encyclopedia of chemical technology- online, 18 May* 2008.

Kosmulski, M. 2006, *Electric Charge Density of Silica, Alumina, and Related Surfaces.*, Encyclopedia of Surface and Colloid Science.

Kosmulski, M., Prochniak, P. & Rosenholm, J.B. 2009, "Electrokinetic potentials of Al_2O_3 in concentrated solutions of metal sulfates", *Journal of colloid and interface science,* vol. 338, no. 1, pp. 316-318.

Krauskopf, K.B. 1956, "Dissolution and precipitation of silica at low temperatures", *Geochimica et Cosmochimica Acta,* vol. 10, pp. 1-26.

Lewis, A.E. & Nathoo, J. 2006, *Contaminant Removal from gas liquor using hydrometallurgical methods*, University 0f Cape Town, South Africa.

Li, L. & Stanforth, R. 2000, "Distinguishing Adsorption and Surface Precipitation of Phosphate on Goethite (α-FeOOH)", *Journal of Colloid and Interface Science,* vol. 230, no. 1, pp. 12-21.

Lippens, B.C. & Steggerda, J.J. 1970, "Active Alumina." in *Physical and chemical aspects of adsorbents and catalysts.*, eds. B.G. Linsen & J.H. de Boer, Academic Press, New York, pp. 171-211.

Lounici, H., Adour, L., Belhocine, D., Elmidaoui, A., Bariou, B. & Mameri, N. 2001, "Novel technique to regenerate activated alumina bed saturated by flouride ions", *Chemical Engineering Journal,* vol. 81, pp. 153-160.

Manning, B.A. & Goldberg, S. 1996, "Modeling competitive adsorption of arsenate with phosphate and molybdate on oxide minerals.", *Soil Science Society of America Journal,* vol. GO, no 1, pp. 121-131.

Matjie, R.H. & Engelbrecht, R. 2007, "Selective removal of dissolved silicon and aluminum ions from gas liquor by hydrometallurgical methods.", *Hydrometallurgy,* vol. 85, pp. 172-182.

Matson, J.V. 1981, *Industrial waste-water reuse by selective silica removal over activated alumina.* , C02F1/28; C02F1/60; C02F1/60; C02F5/08.

Mersmann, A. 2001, *Crystallisation technology handbook.* Second Edition, Marcel Dekker, Inc, United States of America.

Midkiff, W.S. 2002, *Removal of dissolved and colloidal silica.* , C02F 001/58.

Morterra, C. & Magnacca, G. 1996, "A case study: surface chemistry and surface structure of catalytic aluminas, as studied by vibrational spectroscopy of adsorbed species", *Catalysis Today,* vol. 27, pp. 497-532.

Mullin, J.W. 1972, *Crystallisation.* Second Edition, Butterworth Group, England.

Myerson, A.S. 2002, *Handbook of industrial crystallisation.* Second edition, Butterworth-Heinemann., United States of America.

Nielsen, A.E. 1979, Industrial Crystallisation*,* Amsterdam:Jong and Jancic.

Oelkers, E.H. & Jacques, S. 1995, "Experimental study of anorthite dissolution and the relative mechanism of felspar hydrolysis", *Geochimica et Cosmochimica Acta,* vol. 59, pp. 5039-5053.

Okamoto, G., Okura, T. & Goto, K. 1957, "Properties of silica in water", *Geochimica et Cosmochimica Acta,* vol. 12, no. 1-2, pp. 123-132.

Owen, L.B. 1972, *Precipitation of armorphous silica from high-temperature hypersaline geothermal brines.*, Lawrence Livermore Laboratory., University of California.

Peairs, D. 2007, "Silica over-saturation, precipitation, prevention and remediation in hot water systems.", *Cal Water.*

Pelmenschikov, A., Leszczynski, J. & Pettersson, L.G.M. 2001 "Mechanism of dissolution of neutral silica surfaces: Including effect of self-healing.", *Journal of Physical Chemistry A,* vol. 41, pp. 9528-9532.

Peri, J.B. 1965, "Infrared and gravimetric study of the surface hydration of y-alumina", *Journal of Physical Chemistry,* vol. 69, no. 211, pp. 219.

Randolph, A.D. & Larson, M.A. 1988, *Theory of particle processes,* Second edn, Academic Press, New York.

Roelofs, F. & Vogelsberger, W. 2006, "Dissolution kinetics of nano-dispersed γ-alumina in aqueous solution at different pH: Unusual kinetic size effect and formation of a new phase", *Journal of Colloid and Interface Science,* vol. 303, no. 2, pp. 450-459.

Selim, S.A., El Shafei, G.M.S., Mekewi, M., Stone, W.E.E. & Vielvoye, L. 1996, "Effect of partially neutralized aluminum solutions on the texture and pore structure of silica", *Colloids and Surfaces A: Physicochemical and Engineering Aspects,* vol. 117, no. 1-2, pp. 131-141.

Sheikholeslami, R., Al-Mutaz, I.S., Koo, T. & Young, A. 2001, "Pretreatment and the effect of cations and anions on prevention of silica fouling", *Desalination,* vol. 139, no. 1-3, pp. 83-95.

Sheikholeslami, R. & Tan, S. 1999b, "Effects of water quality on silica fouling of desalination plants", *Desalination,* vol. 126, no. 1-3, pp. 267-280.

Sohnel, O. & Garside, J. 1992, *Precipitation.* Butterworth-Heinemann., Great Britain.

Stumm, W. 1997, "Reactivity at the mineral-water interface: dissolution and inhibition", *Colloids and Surfaces A: Physicochemical and Engineering Aspects,* vol. 120, pp. 143-166.

Stumm, W. & Morgan, J.J. 1996, *Aquatic Chemistry: Chemical equilibria and rates in natural waters.* 3rd edn, Wiley- Interscience, United States of America.

Stumm, W. & Morgan, J.J. 1981, *Aquatic Chemistry.* Second Edition, John Willey & Sons, Canada.

Stumm, W. 1992, *Chemistry of the solid-water interface: Processes at the mineral-water and particle-water interface in natural systems,* Wiley-Interscience, New York.

Tejedor-Tejedor, M.I and Anderson, M.A. 1990, "Protonation of phosphate on the surface of goethite as studied by CIR-FTIR and electrophoretic mobility.", *Langmuir,* vol. 6, pp. 602-611.

Ubaldini, S., Massidda, R.:.V., F. & Beolchini, F. 2006, "Gold stripping by hydro-alcoholic solutions from activated carbon: Experimental results and data analysis by semi-empirical model.", *Hydrometallurgy,* vol. 81, pp. 40-44.

van Nierop, P., Erasmus, H.B. & van Zyl, J.W. 2000, *Sasol's achievements in the 20th century as a building block for the 21st*, Sasol Technology, Republic of South Africa.

Van Riemsdijk, W.H., Bolt, G.H., Koopal, L.K. & Blaakmeer, J. 1986, "Electrolyte adsorption on heterogeneous surfaces: adsorption models", *Journal of Colloid and Interface Science,* vol. 109, no. 1, pp. 219-228.

Vogelsberger, W., Schmidt, J. & Roelofs, F. 2008, "Dissolution kinetics of oxidic nanoparticles: The observation of an unusual behaviour", *Colloids and Surfaces A: Physicochemical and Engineering Aspects,* vol. 324, no. 1-3, pp. 51-57.

www.malvern.co.uk, Zeta Potential [Homepage of Malvern Instruments], [Online]. Available: April, 05.

Yokoyama, T., Ueda, A., Kato, K., Mogi, K. & Matsuo, S. 2002, "A Study of the Alumina–Silica Gel Adsorbent for the Removal of Silicic Acid from Geothermal Water: Increase in Adsorption Capacity of the Adsorbent due to Formation of Amorphous Aluminosilicate by Adsorption of Silicic Acid", *Journal of Colloid and Interface Science,* vol. 252, no. 1, pp. 1-5.

Yopps, J.A. & Fuerstenau, D.W. 1964, "The zero point of charge of alpha-alumina", *Journal of Colloid Science,* vol. 19, no. 1, pp. 61-71.

8 APPENDICES

8.1 Appendix A: Raw data for aluminum dissolution in gas condensate

Table 4: Al concentrations in gas condensate during Al dissolution experiment collected as a function of time

Sample ID		Al(ppm)
D	0A	1.73
	1A	8.83
	2A	8.82
	3A	8.40
	4A	7.83
	5A	7.83
	6A	8.76
	7A	7.70
	0B	1.73
	1B	9.04
	2B	9.10
	3B	8.54
	4B	8.34
	5B	8.22
	6B	8.56
	7B	8.14

8.2 Appendix B: Particle size distribution

The particle size distribution was done using a Malvern mastersizer. The Malvern mastersizer gives the information as a volume based histogram together with the particle concentration. The conversion of the volume distribution to the number distribution (N) is as shown below:

Delta L = (0.011298-0.01)/2 = 0.00065

Lbar = 0.01 + (Delta L)/2= 0.01065

N = (Volume %/100) * Particle concentration/ (PI()/6*Lbar^3)

Table 5: Excel spreadsheet for the conversion of volume distribution data to number distribution data obtained during dissolution experiments

Size (um)	Delta L/2	LBar	Volume of particle	Number of Particles
0.01		0.01065	6.32303E-07	0
0.011298	0.00065	0.01203	9.11923E-07	0
0.012765	0.00073	0.01359	1.3152E-06	0
0.014422	0.00083	0.01536	1.8969E-06	0
0.016295	0.00094	0.01735	2.7358E-06	0
0.01841	0.00106	0.01961	3.94547E-06	0
0.0208	0.00120	0.02215	5.6901E-06	0
0.0235	0.00135	0.02503	8.20629E-06	0
0.026551	0.00153	0.02827	1.18354E-05	0
0.029998	0.00172	0.03195	1.7069E-05	0
0.033892	0.00195	0.03609	2.46168E-05	0
0.038292	0.00220	0.04078	3.55039E-05	0
0.043264	0.00249	0.04607	5.12047E-05	0
0.04888	0.00281	0.05205	7.38475E-05	0
0.055226	0.00317	0.05881	0.000106506	0
0.062396	0.00359	0.06645	0.000153605	0
0.070496	0.00405	0.07507	0.00022153	0
0.079648	0.00458	0.08482	0.000319494	0
0.089988	0.00517	0.09583	0.000460783	0
0.101671	0.00584	0.10827	0.000664552	0
0.11487	0.00660	0.12233	0.00095843	0
0.129783	0.00746	0.13821	0.001382257	0
0.146631	0.00842	0.15615	0.0019935	0
0.165667	0.00952	0.17642	0.002875077	0
0.187175	0.01075	0.19932	0.00414649	0
0.211474	0.01215	0.22520	0.005980115	0
0.238928	0.01373	0.25444	0.00862466	0
0.269947	0.01551	0.28747	0.01243867	0
0.304992	0.01752	0.32479	0.017939262	0
0.344587	0.01980	0.36695	0.025872314	0
0.389322	0.02237	0.41459	0.037313509	0
0.439865	0.02527	0.46842	0.05381416	0
0.496969	0.02855	0.52923	0.077611676	0
0.561487	0.03226	0.59793	0.111933058	0
0.634381	0.03645	0.67556	0.16143193	0
0.716738	0.04118	0.76326	0.232820061	0
0.809787	0.04652	0.86235	0.3357775	0

0.914916	0.05256	0.97430	0.484264627	18768829038
1.033693	0.05939	1.10079	0.698414477	91494538194
1.167889	0.06710	1.24370	1.007265488	1.75338E+11
1.319508	0.07581	1.40516	1.452696969	2.00373E+11
1.49081	0.08565	1.58758	2.095105466	1.84264E+11
1.684351	0.09677	1.79368	3.021598721	1.59282E+11
1.903018	0.10933	2.02655	4.357804061	1.29174E+11
2.150073	0.12353	2.28964	6.28490223	1.01174E+11
2.429201	0.13956	2.58688	9.064200142	77182038022
2.744567	0.15768	2.92272	13.07255505	57661700938
3.100874	0.17815	3.30216	18.85347377	42393553016
3.503438	0.20128	3.73085	27.19081107	30832751840
3.958263	0.22741	4.21520	39.2150727	22294042057
4.472136	0.25694	4.76243	56.55669567	16088246832
5.052721	0.29029	5.38070	81.56708809	11616887672
5.708679	0.32798	6.07924	117.6375163	8402423063
6.449795	0.37056	6.86846	169.6589373	6087705347
7.287125	0.41867	7.76014	244.6851582	4418896299
8.233159	0.47302	8.76758	352.8893103	3214130202
9.30201	0.53443	9.90582	508.9432895	2345383159
10.50962	0.60381	11.19182	734.0071776	1721424216
11.87401	0.68219	12.64477	1058.598365	1276325540
13.41553	0.77076	14.28635	1526.729561	960094890.3
15.15717	0.87082	16.14104	2201.876732	736424631
17.12491	0.98387	18.23651	3175.586018	577535894
19.34811	1.11160	20.60402	4579.887342	462527420.8
21.85994	1.25591	23.27890	6605.19596	376289060.2
24.69785	1.41896	26.30102	9526.131999	308848535.8
27.9042	1.60317	29.71549	13738.75838	252791967.3
31.52679	1.81130	33.57324	19814.28418	204698886.6
35.61969	2.04645	37.93181	28576.51654	162721083
40.24393	2.31212	42.85622	41213.56475	126205884.2
45.46851	2.61229	48.41993	59438.94339	95034991.84
51.37135	2.95142	54.70594	85723.91194	69186981.27
58.04052	3.33458	61.80801	123632.5664	48470725.68
65.5755	3.76749	69.83209	178305.11	32567920.69
74.08869	4.25659	78.89788	257154.8323	20898058.97
83.70708	4.80920	89.14062	370873.3167	12735349.24
94.57416	5.43354	100.71310	534880.159	7314527.739
106.852	6.13894	113.78795	771413.7663	3910641.645
120.7239	6.93591	128.56020	1112546.793	1911290.971
136.3966	7.83635	145.25024	1604534.979	826624.3909
154.1039	8.85369	164.10702	2314089.161	283254.7039

174.1101	10.00309	185.41184	3337420.933	49083.63173
196.7136	11.30172	209.48250	4813288.414	0
222.2514	12.76894	236.67809	6941811.03	0
251.1047	14.42664	267.40428	10011604.5	0
283.7038	16.29955	302.11943	14438915.79	0
320.535	18.41560	341.34139	20824063.73	0
362.1478	20.80636	385.65526	30032838.76	0
409.1628	23.50750	435.72207	43313899.54	0
462.2814	26.55931	492.28869	62468083.94	0
522.296	30.00731	556.19894	90092592.57	0
590.1019	33.90294	628.40619	129933155.1	0
666.7105	38.30431	709.98758	187391930.1	0
753.2647	43.27708	802.16010	270260007.2	0
851.0555	48.89543	906.29869	389773836.7	0
961.5419	55.24317	1023.95685	562138828.4	0
1086.372	62.41498	1156.88970	810726713.9	0
1227.408	70.51787	1307.08025	1169244628	0
1386.753	79.67269	1476.76895	1686305604	0
1566.785	90.01601	1668.48710	2432020228	0
1770.189	101.70214	1885.09462	3507503256	0
2000	114.90538	2000.00000	4188790205	0
				1.34987E+12

8.3 Appendix C: Raw data for silica zeta potential in 0.01M NaCl

Table 6: Silica zeta potentials obtained when using 0.01M NaCl

pH	Zeta potential(mV) Reading 1	Reading 2	Reading 3	Average
1.87	-24.00	-26.50	-28.80	-26.43
2.14	-28.20	-27.60	-27.90	-27.90
2.68	-33.30	-32.30	-33.80	-33.13
3.05	-36.50	-37.60	-37.90	-37.33
3.86	-39.70	-42.90	-39.60	-40.73
4.15	-40.80	-42.40	-43.60	-42.27
5.55	-40.50	-37.50	-41.30	-39.77
8.35	-52.30	-52.60	-54.20	-53.03
8.70	-53.30	-55.00	-58.30	-55.53
8.89	-55.50	-58.90	-60.80	-58.40
9.13	-56.50	-56.70	-60.60	-57.93
9.70	-53.70	-57.30	-58.80	-56.60
10.04	-54.60	-57.70	-58.40	-56.90

8.4 Appendix D: Results for alumina loading with aluminosilicate species

For the alumina loading experiments, two samples were collected at a given time during the experiments. The graphs were plotted using the average concentration of the two samples. Thus, the results presented in this thesis for alumina loading are an average of the two samples collected at regular intervals. However, a similar trend in the removal of the aluminosilicate species was observed during the experiments. The species removal was calculated using the following equation:

$$\% \text{ Species removal} = \frac{\left(C_{initial} - C_{final}\right)}{C_{initial}} \times 100$$

For example % Si removal after treating 180ml of gas condensate will be calculated as follows:

$C_{initial}$ = (8.90+9.53)/2 = 9.22

C_{final} = (2.05+2.09)/2 = 2.07

%Si removal = ((9.22-2.07)/9.22) x 100%

= 77.55%

Table 7: Concentrations of Si, Ca and Al in gas condensate continuously fed through a packed bed of activated alumina

Sample ID		Cumulative Volume of gas condensate treated	Al(ppm)	Ca(ppm)	Si(ppm)
CN12	0A	0	2.13	1.87	8.90
	1A	180	4.42	0.55	2.05
	2A	360	5.48	0.32	1.39
	3A	540	7.20	0.35	1.35
	4A	1080	8.75	0.40	1.74
	5A	2160	9.78	0.48	1.93
	6A	3240	10.32	0.60	2.08
	7A	4320	10.49	0.60	2.29
	8A	6480	11.38	0.72	2.66
	9A	8100	11.45	0.81	2.78
	10A	Overall	10.62	0.66	2.34
	0B	0	1.94	1.87	9.53
	1B	180	4.18	0.58	2.09
	2B	360	5.58	0.33	1.38
	3B	540	6.75	0.33	1.40
	4B	1080	8.78	0.39	1.70
	5B	2160	9.33	0.68	1.89
	6B	3240	10.21	0.58	2.19
	7B	4320	10.66	0.60	2.26
	8B	6480	11.34	0.75	0.91
	9B	8100	10.74	0.81	1.48
	10B	Overall	10.37	0.67	1.77

8.5 Appendix E: Regeneration data for selected experiments to show calculations and reproducibility of the experimental results

The amount of species removed from the stream by alumina was calculated using the overall concentration.

Sample calculation:

For the data given on the following table, the amount of Si loaded/adsorbed will be calculated as follows:

Amount of Si adsorbed $= (\text{Initial} - \text{Overall})_{\text{Average Concentration}} \times \text{Total volume}/1000$

$= (7.95 - 1.10) \times 8640/1000$

$= 59.18\text{mg}$

Percentage Si desorbed will be then calculated using the following equation:

$$\%\ \text{Species unloaded} = \frac{\text{Mass in effluent}}{\text{Mass initial adsorbed}} \times 100$$

Where mass in effluent = Concentration x Volume of reagent used

Table 8: Concentrations of Si, Ca and Al in gas condensate continuously fed through a packed bed of activated alumina

Sample ID		Cumulative Volume of gas condensate treated	Al(ppm)	Ca(ppm)	Si(ppm)
CN21	0A	0	1.45	1.41	7.95
	1A	180	3.62	0.21	0.54
	2A	360	4.58	0.21	0.59
	3A	720	5.82	0.22	0.62
	4A	2160	7.32	0.34	1.00
	5A	4320	7.85	0.42	0.99
	6A	6480	7.75	0.49	0.68
	7A	8640	7.33	0.62	1.09
	8A	Overall	7.45	0.45	1.09
	0B	0	1.42	1.39	7.95
	1B	180	3.80	0.22	0.55
	2B	360	4.54	0.21	0.59
	3B	720	6.09	0.23	0.65
	4B	2160	7.65	0.34	1.03
	5B	4320	8.00	0.40	1.02
	6B	6480	7.54	0.47	0.94
	7B	8640	7.43	0.60	1.16
	8B	Overall	7.86	0.48	1.10

The unloading experiments were repeated 2 times after a first run was done to investigate the general trend in species evolution for the two regenerants (NaOH and sulphuric acid). The graph below show the results obtained and that the results were reproducible. Thus, the results presented in this thesis are an average of the results obtained when loaded alumina was divided into equal portions after loading and then regenerated under the same experimental conditions. It is apparent that the desorbable Si was complete after 15 minutes. The difference in the concentrations could be as a result of analysis errors and the complexity of silica reactions in the presence of other species especially aluminum.

Table 9: Concentrations of Si, Ca and Al in liquid samples during continuous regeneration of loaded alumina with 0.1M H_2SO_4

	Run 1	**Run 2**	
Time (minutes)	**Average Si(ppm)**	**Average Si(ppm)**	**Average (ppm)**
0	0.00	0.00	0.00
5	6.88	6.97	6.93
10	15.72	13.99	14.85
15	13.70	11.48	12.59
20	9.87	11.02	10.44
30	6.73	7.57	7.15
45	4.93	5.29	5.11
60	3.77	4.17	3.97
90	2.76	3.20	2.98
120	1.96	2.26	2.11

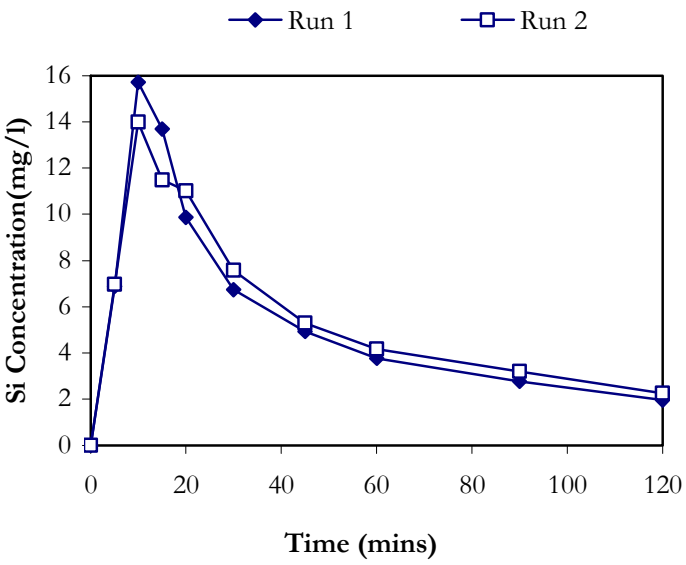

Figure 45: Concentrations of Si removed from loaded alumina in washing solution attained when using 0.1M H_2SO_4 for two different runs (3 minutes residence time)